Competence Centre Directorate

HUY.EADS.MIS.RE.0002

TE311 n° 143 085
Issue 1 - 22 December 2004
Page 1

HUYGENS PROGRAM

ENTRY MODULE AERODYNAMIC DATABASE

DISTRIBUTION

- Of the document:

ALCATEL Space	(8)	Mme	SCHIPPER
TO72		M.	PLOTARD
TE31		M.	PAULAT
TE311	(2)	M.	TRAN
		ALTRAN (TE311 contract)	
TE321		M.	BRENNER
TO7		Mme	PONS
TA413			

- Of the identification sheet, of the abstract and of this distribution list:

TE311	M.	FOURURE
TE31	M.	LELEU

EADS SPACE TRANSPORTATION

Internal reference : TE311 143 085	**Issue**	**Rev.**	**Date :**	22.12.04
Structured reference : HUY.EADS.MIS.RE.0002	1		**Page**	3/51

CLASSIFICATION	**COMPANY**		**MILITARY**			**PROGRAMME**		
	EADS-ST unprotected	[X]	Unclassified	(NP)	[X]	General Public	(1)	[ ]
	EADS-ST Reserved	[ ]	Confidential	(CD)	[ ]	Industry	(2)	[ ]
	EADS-ST Confidential	[ ]	Secret	(SD)	[ ]	Restricted	(3)	[ ]
	EADS-ST Secret	[ ]	Top Secret	N/A		Confidential	(4)	[ ]
	Restricted (DR)	[ ]	French National	(SF)	[ ]			

CONTRACT	**Customer**	**Contract number**			**Programme**
	ALCATEL Space				HUYGENS
	Contractual doc[t] yes [X] no [ ]	C.Work Unit	Item	Sub-item	**CWS**
	as requested [ ] as per CWS [ ]				**WP**

TITLE HUYGENS PROGRAM
ENTRY MODULE AERODYNAMIC DATABASE

ABSTRACT

This report describes the up-dating of the Huygens Entry Module AErodynamic DataBase (AEDB). FFA Wind Tunnel Test results at M = 7 have been removed and replaced by Navier-Stokes computation results. Only the axial force coefficient at Mach 7 and above has been modified compared to the previous AEDB, resulting in lower values.

KEYWORDS

- HUYGENS - ENTRY MODULE - ENTRY PHASE - AERODYNAMICS

File ref. : C24342/VAL **Software** : XP		**Configuration management**		**Distribution category**	
Language code : ENG **Taking precedence** : FR		None [ ] Internal [ ]		**Interest**	Short term [ ] Medium or long term [X]
30 figures	5 appendices	Customer [ ]		**Sup. distribution**	Authorized [X] Checked [ ]

VISAS	**Authors**	**Controller**	**Quality**	**Section Manager**	**Department Head**
Sigle	TE311 - ALTRAN	TE31		TE311	TE31
Name	Ph. TRAN S. LENOIR	J.C. PAULAT		B. FOURURE	F. LELEU
Signature					

ISSUE / REVISION STATUS RECORD		
Issue and revision n°	**Date**	**Main reasons for document change (+ paragraphs nb concerned in case of revision) Document validity status (reference and date)**
Issue 1	22.12.04	Original document

ABSTRACT

SECTION: TE311 **NUMBER:** 143 085 **DATE:** 22.12.04

AUTHOR(S): Ph. TRAN - ALTRAN (TE311 contract)

TITLE: HUYGENS PROGRAM
ENTRY MODULE AERODYNAMIC DATABASE

The EM AEDB has been modified according to the Delta-FAR recommendations held on February 3rd and 4th, 2004. The FFA WTT data at M = 7.15 have been removed since they were believed to be not sufficiently reliable. But for time and cost reasons, no WTT campaign was performed in order to provide with up-dated aerodynamic coefficients at M = 7.15, and CFD mean was used to address this issue. A very limited set of computations was performed: M = 4, $\alpha = 0°/10°$ and M = 7.15, $\alpha = 0°/10°/20°/30°$ in FFA WT conditions and a M = 10, $\alpha = 0°$ case for verification. Only perfect gas $\gamma = 1.4$ cases were computed by EADS-ST. ESA provided some complementary results including reactive gas effects.

CFD analysis indicates that axial coefficient was questionable and only this coefficient was corrected in the EM AEDB by reducing its nominal value by approximately 4% (at $\alpha = 0°$, C_D is reduced from 1.54 down to 1.48). This nominal value is then kept constant for Mach numbers above M = 7.15. This assumption is not in contradiction with the ESA reactive gas computations results. C_N and C_m coefficients may be affected by real gas effects, but this has not been accounted for in the present up-dating, since the current values are believed to be conservative (less statically stable EM) and applicable for design. A review of rarefaction effect has been performed. DSMC computations were performed in 1992 and used to correct the Cm pitching moment coefficient for Knudsen numbers ranging between 10^{-3} and 10. C_A axial coefficients were found to be affected by rarefaction effects but no correction was applied to that parameter, since no impact on the global deceleration profile was expected.

The up-dated AEDB is then assessed in terms of flight mechanics. The impact on the EM during entry is negligible. The dynamic pressure and the angle-of-attack at PDD instant are also weakly affected while the Mach number at PDD tends to be slightly lower than that predicted with the previous 1993 AEDB. All these parameters remain in the EM design range.

Due to the very limited set of computations, the up-dated AEDB (unlike the previous one) is preferably used for **design** issues, since real gas and rarefaction effects have been only poorly described. For **prediction** purposes, it is necessary to improve the following issues:

- drag force coefficient in transitional regime, to which past DSMC results indicated possible discrepancies. This may have an impact on the analysis of the accurate accelerometers measurements as installed in the HASI instrument. Complementary DSMC computations would be useful to that respect.

- forces and moments coefficients at high hypersonic regime. More exhaustive computations with reactive gas assumption would be useful. However, since a strong uncertainty is associated to this kind of results because of the lack of reliable experimental data, mesh refinement and code cross-checking tasks are strongly required. The European ARD flight may be used as a preceeding verification of the CFD code reactive gas capabilities. More ambitious would be to plan WTT campaign (forces & moments) in high enthalpy facilities like F4 or even HEG.

Section Manager of TE311

B. FOURURE

Summary

1. REFERENCES

[R1] Measurement of Static Stability Characteristics and Base Pressure Coefficients on an Entry Module with Flat and Ordinary Back Cover of Cassini/Huygens Space Probe in the FFA Transonic/Supersonic and Hypersonic Wind Tunnels S4 and Hyp500
Lennart HJELMBERG
FFA TN 1993-15

[R2] HUYGENS Program
Descent and Entry Module AErodynamic Static DataBase
HUY-AS/m-120-PL-0007
TAQUIN G. - BLANCHET D.
22 June 1993

[R3] HUYGENS Program
Uncertainty on Entry Module Axial Force Coefficient
HUY-AS/m-120-TN-0018
BAILLION M.
11 July 1994

[R4] HUYGENS Program
Entry, Descent and Thermal Analyses
HUY.EADS.HIT.RE.002
PEREZ S. - VILLAUMIE K. - TRAN Ph. - GARSAULT N. - DUPILLIER J.M.
May 2004

[R5] HUYGENS Program
Recovery Implementation Tasks: Entry and Descent Specifications for EADS Trajectory Simulations: HUYGENS New Baseline Mission and Titan Gravity Waves
HUY.ASPI.HIT.SP.0003 Issue 1.0
5 August 2003

[R6] HUYGENS Program
Phases B'2/B3 Aerodynamic Studies
HUY-AS/m-120-TN-0009
31 August 1992

[R7] HUYGENS Program
Entry Module Dynamic Database
HUY-AS/m-120-TN-0018
24 July 1995

2. INTRODUCTION

This document presents an up-date of the Huygens Entry Module (EM) AErodynamic DataBase (AEDB). This up-date results from the Delta-FAR recommendations held on February 3rd and 4th, 2004. The FFA Wind Tunnel Tests at Mach 7.15 were believed to introduce a bias onto the AEDB at least on the axial force coefficients. This issue is identified in the present document and corrective actions have been applied. It was decided to remove the FFA WTT results from the current AEDB and to replace them by CFD results. As a result, an up-dated AEDB for the Huygens EM is proposed. Due to the very limited set of computations, the up-dated AEDB (unlike the previous one) is preferably used for design issues, since real gas and rarefaction effects have been only poorly described.

3. ENTRY MODULE REFERENCE SHAPE

The Huygens EM reference shape is presented in figure 1 and numerical values in table 1.

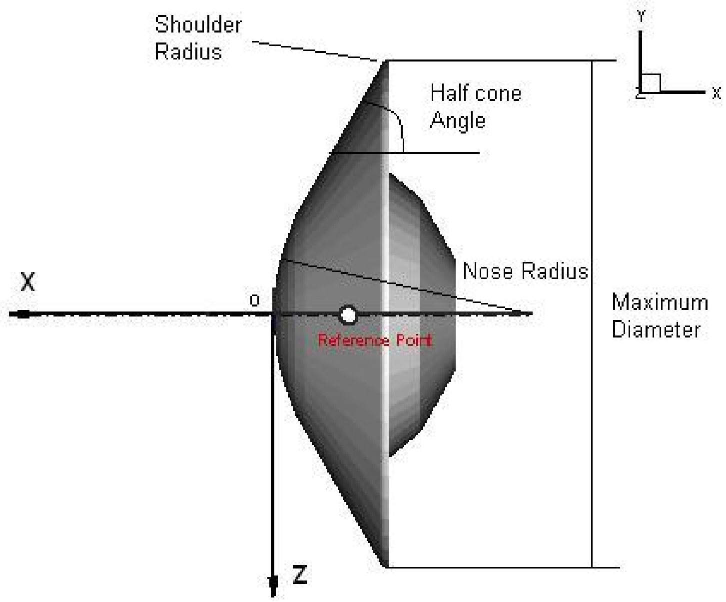

FIGURE 1 - HUYGENS SHAPE GEOMETRY

Maximum diameter/Reference Length	2.7 m
Nose radius	1.2501 m
Heat shield half cone angle	60°
Shoulder radius	0.0486 m
Reference surface	5.73 m^2
Moment Reference Center (MRC)	X_{ref}/L_{ref} = - 0.265 Y_{ref}/L_{ref} = 0 Z_{ref}/L_{ref} = 0

TABLE 1 - ENTRY MODULE SHAPE DIMENSIONS AND REFERENCE QUANTITIES

The Mass, Centering and Inertia (MCI) characteristics are given in the following table:

Mass	320 kg
Center of Gravity	X_{CoG} = - 471.76 mm Y_{CoG} = 1.53 mm Z_{CoG} = 4.93 mm
Ixx	127.97 kg.m²
Iyy	75.85 kg.m²
Izz	71.9 kg.m²
Ixy	0.45 kg.m²
Iyz	0.338 kg.m²
Ixz	-0.096 kg.m²

TABLE 2 - ENTRY MODULE MCI

4. REFERENCE AXES

Two reference axes systems are considered and described in the following figure:

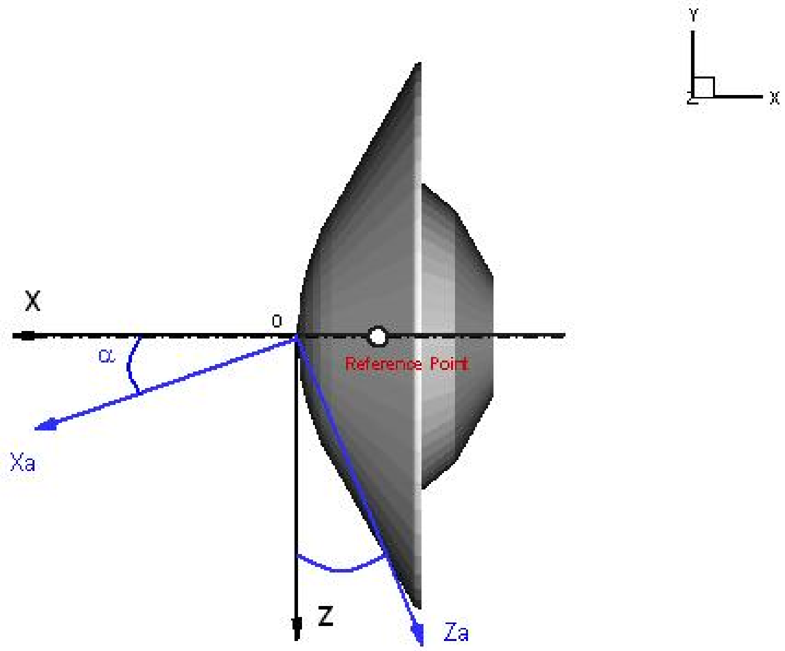

FIGURE 2 - HUYGENS REFERENCE AXES SYSTEMS

- the first system is the body-fixed axes system. The X-axis is the symmetry axis of the axisymmetric shape, directed forward, and the Z-axis is perpendicular and directed to the bottom of the capsule.

- the second system is the velocity-fixed axes system. The Xa-axis is along and in the direction of the velocity and the Za-axis is the perpendicular.

The origin of these axes systems is arbitrarily set at the nose of the capsule. These two systems can be deduced from each other by the angle-of-attack α, positive when the Z-component of the velocity, in the body-fixed system, is positive.

5. AERODYNAMIC COEFFICIENTS DEFINITION

In the velocity-fixed system, we have:

- C_D: drag coefficient,
- C_L: lift coefficient.

In the body-fixed system, we have:

- C_A: axial force coefficient,
- C_N: normal force coefficient,
- C_{mMRC}: pitching moment coefficient at the Moment Reference Center point (MRC).

This pitching moment coefficient may be transferred at any other point of the module with the following formula which is written for the Center of Gravity and the Moment Reference Center from tables 1 and 2:

$$C_{mCoG} = C_{mMRC} - \frac{Z_{MRC} - Z_{CoG}}{L_{ref}}.C_A + \frac{X_{MRC} - X_{CoG}}{L_{ref}}.C_N$$

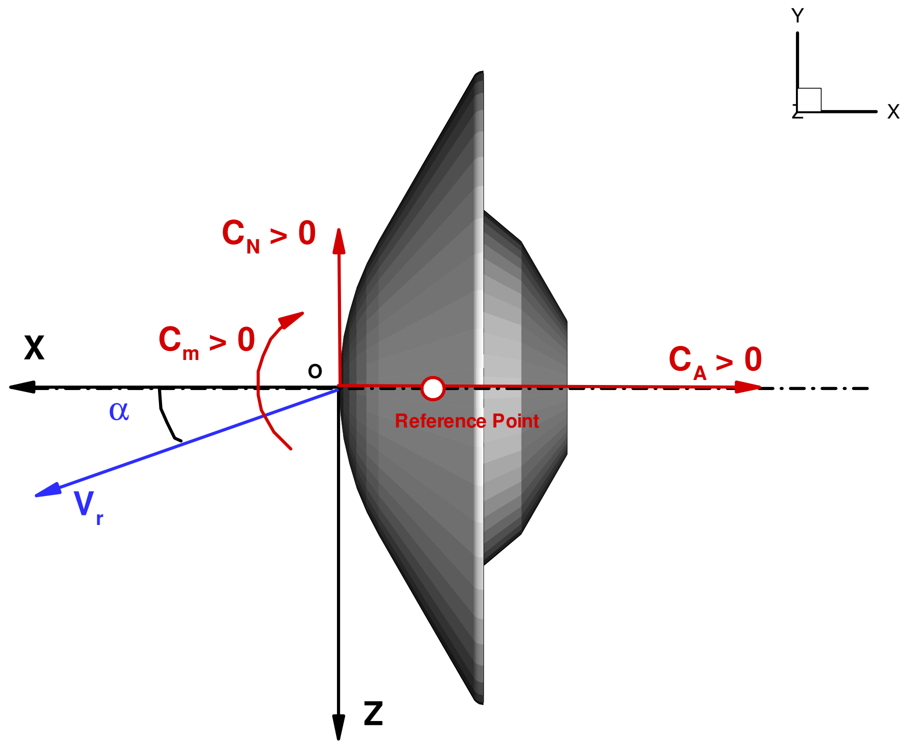

FIGURE 3 - HUYGENS AERODYNAMIC COEFFICIENTS CONVENTION

where:

- α is the total angle-of-attack in degree,
- Vr is the velocity of the probe relative to the atmosphere.

These coefficients are linked by the following relations:

- $C_D = C_A.\cos\alpha + C_N.\sin\alpha$
- $C_L = -C_A.\sin\alpha + C_N.\cos\alpha$
- $C_A = C_D.\cos\alpha - C_L.\sin\alpha$
- $C_N = C_D.\sin\alpha + C_L.\cos\alpha$

We can here introduce the center-of-pressure location definition: this is the point where the aerodynamic forces do apply. This value is given in percent of the reference length and is positive toward the base (i.e. opposite to X-axis). Its origin stands at the nose. In equation, this would be:

$$x_{CP} / L_{ref} = -100.(X_{MRC} + L_{ref}.\frac{C_{mMRC}}{C_N}) / L_{ref}$$

where:

- x_{CP} is the abscissa of the center-of-pressure location (positive toward the base),
- X_{MRC} is the abscissa of the Moment Reference Center.

6. CFD ANALYSIS

6.1 FOREWORD

Delta-FAR recommendations resulted in re-examining the previous EM AEDB at and above Mach 7.15 for which unconsistencies compared to some CFD analysis results were identified. Aerodynamic coefficients were based on computations (Euler or Navier-Stokes solutions) and Wind Tunnel Tests (WTT) performed in the Swedish FFA facility. But, it must be pointed out that FFA WT results at Mach 7.15 were already believed questionable during the development phase as pointed out in document [R2], but included however in the AEDB as an upper value.

Finally, only hypersonic values are questionable ($M \geq 7.15$): values for $M \leq 4$ are well correlated with the FFA Wind Tunnel experiments and CFD analysis results (see [R2]) and so do not need to be modified.

It was not possible to perform complementary WTT for time and cost reasons, and CFD results must be trust. A first computation is performed at M = 4 in FFA WT conditions in order to assess the validity of the CFD code, then computation at M = 7.15 under FFA WT conditions was performed; the result is then corrected from M = 4 WTT/CFD differences in order to derive the "best estimate" aerodynamic coefficients set. Note that only cold hypersonic regime is considered.

6.2 CFD HYPOTHESIS

Navier-Stokes computations using FLUSEPA code have been realized in the FFA Wind Tunnel conditions. Following assumptions are used:

- the flow regime is laminar,
- the gas is considered as perfect gas : $\gamma = 1.4$,
- wall temperature is 290 K.

Computations have been performed for 3 Mach numbers, M = 4 ($\alpha = 0°$, $10°$) and 7.15 ($\alpha = 0°$, $10°$, $20°$, $30°$) in FFA WT conditions and M = 10 ($\alpha = 10°$) for a Mach effect assessment:

M_∞	P_∞ (Pa)	T_∞ (K)	V_∞ (m/s)	Rho_∞ (kg/m^3)	$Re_{\infty D}$
4	9 000	89	758	0.350892	5.20E+06
7.15	1 900	57	1 084.3	0.115664	3.80E+06
10.21	1 900	57	1 549	0.115664	5.40E+06

TABLE 3 - NAVIER-STOKES SIMULATIONS HYPOTHESES

An unstructured mesh was used. The grid mesh was filled with 38.700 cells in 2D and 936.000 cells in 3D (see appendix 1). Particular attention has been paid on the bow shock capture and on the boundary-layer development description to which a y+ of 1 was set. The expansion at the shoulder plays an important role in the aerodynamic coefficients determination and the surface grid has also been refined in this region. The wake region has been described by extending the computational domain by a factor 5 x D downstream.

6.3 NUMERICAL RESULTS

Table 4 sums up the results of the different CFD Navier-Stokes calculations:

Mach	4		7,15				10
angle-of-attack (°)	0	10	0	10	20	30	0
C_A	1.472	1.4382	1.455	1.3955	1.229	1.05	1.456
C_N	0	0.0452	0	0.05164	0.1159	0.1656	0
C_m (MRC)	0	- 0.0191	0	- 0.02156	- 0.0522	- 0.0775	0

TABLE 4 - NAVIER-STOKES SIMULATIONS RESULTS

Pressure coefficient and Mach number fields obtained with Navier-Stokes calculations are illustrated in appendices 2 and 3. One can observe the presence of a recompression shock at the back-cover at $\alpha = 0°$. This phenomenon is believed to be due to a numerical artefact; an only slight increase of the incidence and the shock would vanish. However, this sensitivity analysis has not been performed in the present document.

Figures 4 to 6 present the comparison between the values from the previous data base and the values obtained with CFD computations and FFA Wind Tunnel Tests at M = 4. Very good agreement is achieved on C_A, C_N and Cm coefficients. For the last parameter, a slight shift of the experimental value is due to an experimental bias; it should be zero at 0° incidence. This excellent comparison at M = 4 adds confidence to the CFD analysis and the M = 7.15 case can be then performed. Figures 7 to 9 present the comparison at M = 7.15. WTT/CFD differences are larger at M = 7.15 than at M = 4 as expected, particularly on the C_A coefficients. WTT nominal data are close to the upper bound of the AEDB while CFD data are closer to the lower bound. On C_N and C_m coefficients, lower differences are observed. Navier-Stokes computations show a less statically stable EM than the AEDB.

Additional ESA 2D axisymmetrical CFD analysis are provided, they have been computed with a reactive gas assumption for high Mach numbers ranging between 14 and 22. A computation at M = 19.6 at 5° of incidence is also available. Since high Mach number AEDB is supposed to be that at M = 7, comparison between ESA and EADS-ST computations makes sense. A good agreement with EADS-ST perfect gas results is observed on C_A. Reactive gas effects are observed on C_N and C_m, for which a more statically stable EM is predicted. This phenomenon has been recently explained by a variation of the pressure distribution on the front-shield due to gas dissociation effects associated to the sonic line motion along the forebody with incidence.

C_A coefficient seems then to be over-estimated in the current AEDB above M = 7, and correction would be brought. AEDB C_N and C_m coefficients are less questionable above M = 7: perfect gas computations indicating a less static stability while reactive gas computation seems to show more static stability. This issue should be addressed in a next phase where more exhaustive reactive gas computations should be performed. Finally, as far as the EM design AEDB is concerned, only axial force coefficient at and above M = 7 is corrected. By eliminating the FFA WTT results, the C_A values will be naturally shifted down if CFD results are valid. A corrective factor has been derived from M = 4 WTT/CFD data comparison and applied at M = 7.15. C_N and C_m coefficients are unchanged.

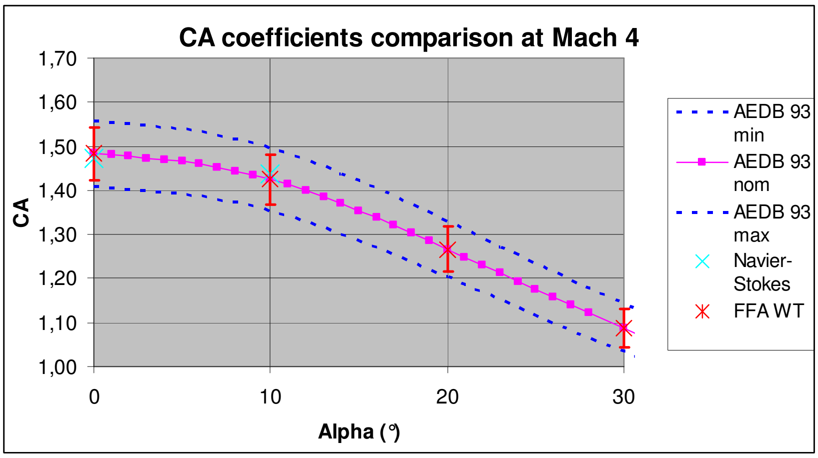

FIGURE 4 - TEST AND CFD COMPUTATIONS VS. PREVIOUS AEDB FOR AXIAL FORCE COEFFICIENT AT MACH 4

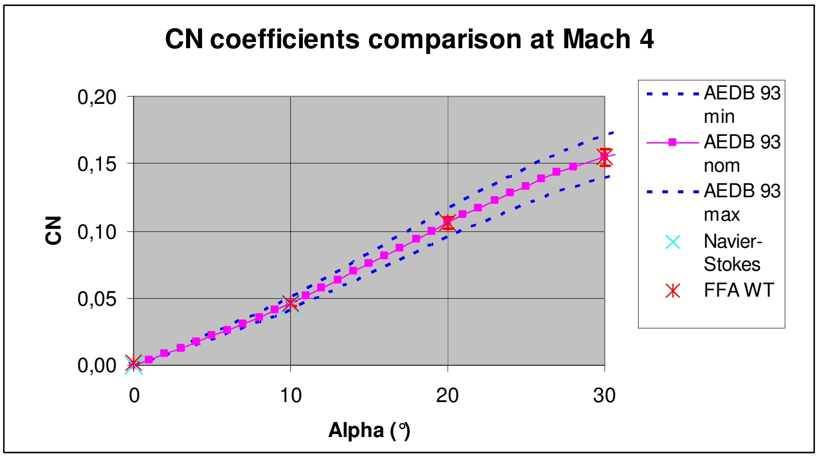

FIGURE 5 - TEST AND CFD COMPUTATIONS VS. PREVIOUS AEDB FOR NORMAL FORCE COEFFICIENT AT MACH 4

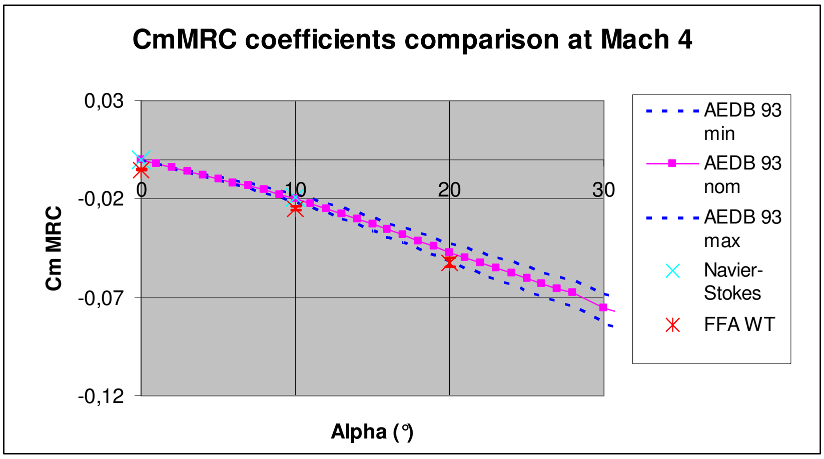

FIGURE 6 - TEST AND CFD COMPUTATIONS VS PREVIOUS AEDB FOR PITCHING MOMENT COEFFICIENT AT MRC AND AT MACH 4

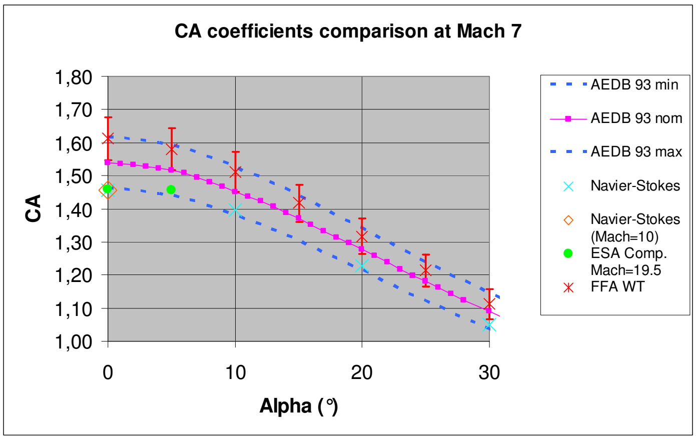

FIGURE 7 - TEST AND CFD COMPUTATIONS VS. PREVIOUS AEDB FOR AXIAL FORCE COEFFICIENT AT MACH 7

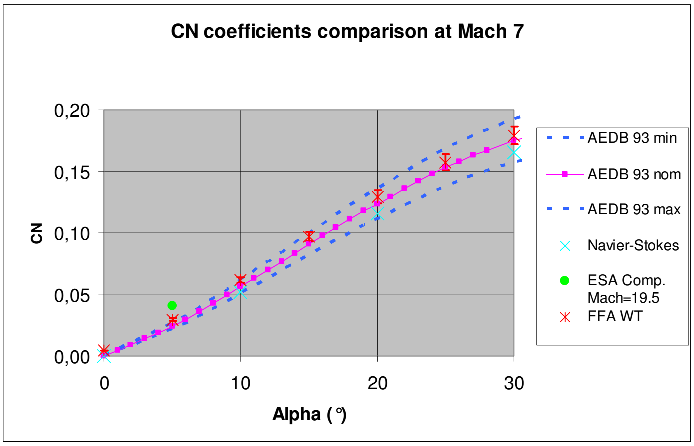

FIGURE 8 - TEST AND CFD COMPUTATIONS VS. PREVIOUS AEDB FOR NORMAL FORCE COEFFICIENT AT MACH 7

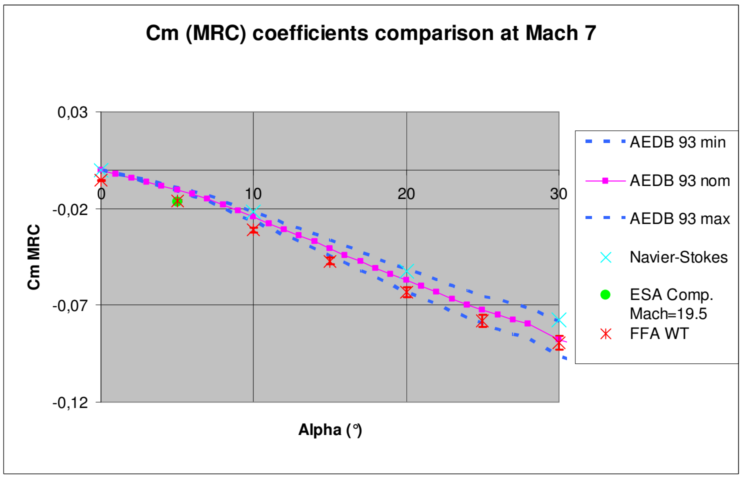

FIGURE 9 - TEST AND CFD COMPUTATIONS VS. PREVIOUS AEDB FOR PITCHING MOMENT COEFFICIENT AT MRC AND AT MACH 7

7. AERODYNAMIC DATABASE (AEDB)

7.1 PRELIMINARY COMMENT

The previous EM AEDB is taken from documents [R2] and [R6].

C_A, C_N, C_m and C_{mq} aerodynamic static and dynamic coefficients are provided in the 3 flow regimes: continuum, transitional and free molecular.

7.2 AERODYNAMIC COEFFICIENTS IN CONTINUUM FLOW

In continuum flow, the aerodynamic coefficients are provided versus:

- Mach number M: the range is [0;99], the coefficients being constant for $M \geq 7$,
- angle-of-attack: the range is [0°;90°].

7.3 AERODYNAMIC COEFFICIENTS IN FREE MOLECULAR FLOW

In free molecular flow regime, the aerodynamic coefficients are function of the angle-of-attack only. They have been calculated at M = 20 and the angle-of-attack range in that case is [0°; 30°]. They are given in the following table:

ALPHA	0	5	10	20	30
C_A	2.09	2.075	2.033	1.864	1.599
C_N	0	0.138	0.272	0.514	0.697
X_{CP}/L	0.211	0.211	0.211	0.211	0.211
C_{mMRC}	0.000000	0.007452	0.014688	0.027756	0.037638

TABLE 5 - FREE MOLECULAR FLOW AERODYNAMIC COEFFICIENTS VS. α

7.4 AERODYNAMIC COEFFICIENTS IN TRANSITIONAL FLOW

In transitional flow (*trans*), the coefficients are interpolated between the continuum regime (*cont*) and the free molecular one (*FMF*). Following *Bridging Function* applies:

$$C_{trans} = C_{cont} + f(Kn).(C_{FMF} - C_{cont})$$

with:

- $C = C_A$, C_N or C_m
- Knudsen Number: $Kn = \sqrt{\frac{\gamma\pi}{2}} * \frac{M_\infty}{\mathrm{Re}_{\infty D}}$.

We considered the flow regime as transitional when the Knudsen Number ranges between [0.001; 10]. Using those bounds, we have the relations:

- continuum flow Kn < 0.001 $f(Kn) = 0$,
- transitional flow 0.001 ≤ Kn ≤ 10 $f(Kn) = \sin^2((3 + \log Kn).\frac{\pi}{8})$,
- free molecular flow Kn > 10 $f(Kn) = 1$.

DSMC (Direct Simulation Monte-Carlo) have been realized to correlate the results found with this bridging function (see document [R6]). Differences were observed on the C_A and the X_{CP}/L_{ref} parameter mainly, but only the latter parameter has been modified since the differences on C_A coefficient were thought to have a negligible impact on the EM deceleration profile (see document [R6]). Consequently, correcting factors have been then introduced on the X_{CP}/L_{ref} (and so C_m) coefficient only depending on the Knudsen number.

Finally, the AEDB numerical values are provided in appendix 5.

The resulting aerodynamic coefficients in transitional flow are plotted in the following figures:

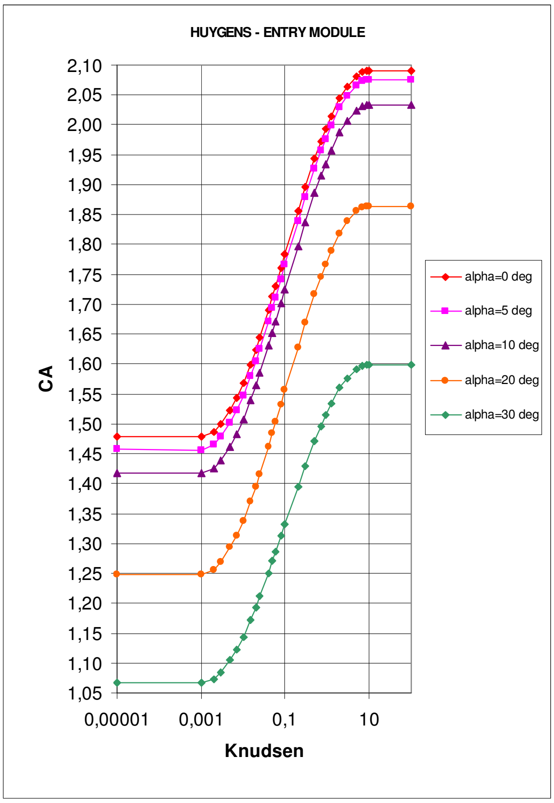

FIGURE 10 - C_A COEFFICIENTS VERSUS KNUDSEN NUMBER AND α

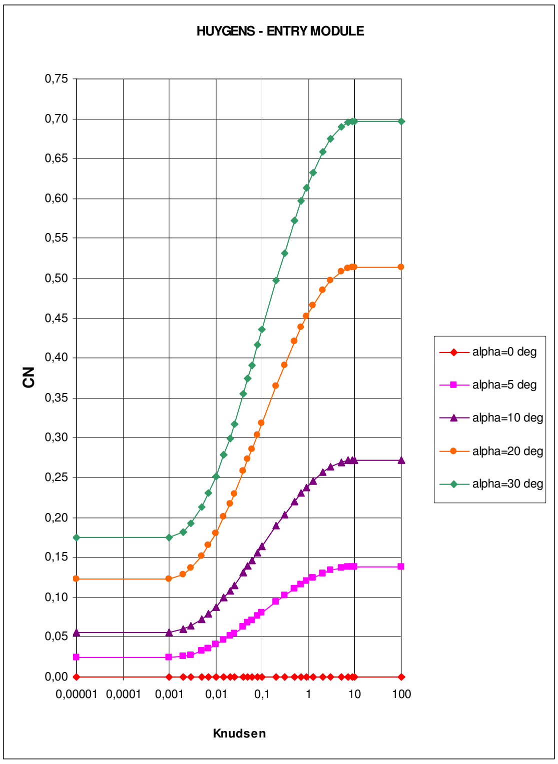

FIGURE 11 - C_N COEFFICIENTS VERSUS KNUDSEN NUMBER AND α

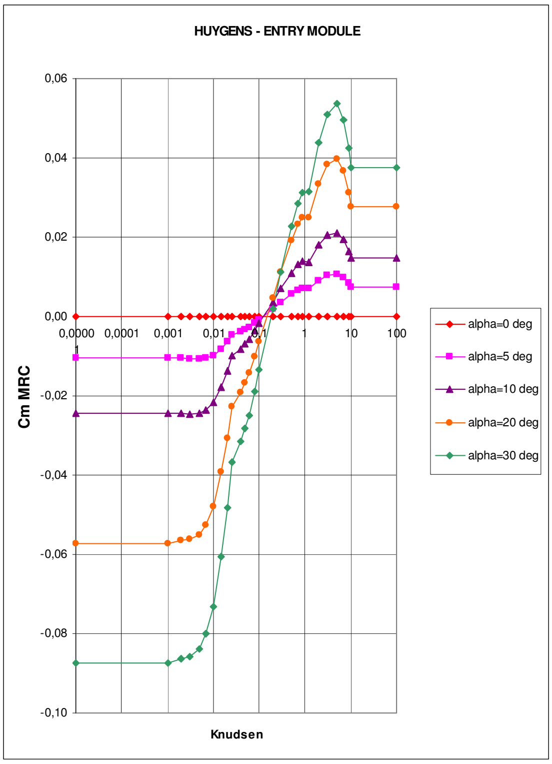

FIGURE 12 - C_{mMRC} COEFFICIENTS VERSUS KNUDSEN NUMBER AND α

7.5 DYNAMIC COEFFICIENT

The pitch damping coefficient derivative $Cm_q + Cm_{\dot{\alpha}}$ is written:

$$Cm_q + Cm_{\dot{\alpha}} = \frac{\partial Cm}{\partial(\frac{q.D}{V_\infty})} + \frac{\partial Cm}{\partial(\frac{\dot{\alpha}D}{V_\infty})}$$

This coefficient is given for the Mach number range [0;100] and angle-of-attack range [0°; 90°] (see document [R7]) and applies whatever the flow regime. However, this parameter plays an important role at Pilot Device Deployment (PDD) instant in supersonic regime (M < 3). The reference point for this parameter is the Center of Gravity (X_{CoG}/D = - 0.17).

7.6 UNCERTAINTIES

The uncertainties associated with the aerodynamic coefficients of the database are:

- C_A ± 5%,
- C_N ± 10%,
- C_m ± 10%,
- C_{mq} No additional uncertainties should be added since the provided AEDB already includes conservative values.

7.7 DIGITAL DATABASE

The database for the Entry Module of Huygens is provided in a form of an Excel file. There are six sheets: four for the continuum flow (C_A, C_N, C_m and C_{mq}), one for the transitional flow regime and one for the free molecular flow regime. We can describe each of them:

- ***Cont_C$_A$***: it is the C_A coefficient in continuum flow. First there are a few lines presenting the reference quantities and then the table of the axial force coefficient. The columns are for the Mach numbers and the lines for the angles-of-attack.

- ***Cont_C$_N$***: it is the C_N coefficient in continuum flow. First there are a few lines presenting the reference quantities and then the table of the normal force coefficient. The columns are for the Mach numbers and the lines for the angles-of-attack.

- ***Cont_C$_m$***: it is the C_m coefficient in continuum flow. First there are a few lines presenting the reference quantities and then the table of the pitching moment coefficient. The columns are for the Mach numbers and the lines for the angles-of-attack.

- ***Cont_C$_{mq}$***: it is the dynamic C_{mq} coefficient in continuum flow. First there are a few lines presenting the reference quantities and then the table of the dynamic pitching moment coefficient. The columns are for the Mach numbers and the lines for the angles-of-attack.

- ***Transitional_flow***: the sheet concerning the transitional flow regime gathers four aerodynamic coefficients: C_A, C_N, X_{CP}/L and C_m. For each of them, there are transitional coefficients versus Knudsen number for five angles-of-attack 0°, 5°, 10°, 20° and 30°. Coefficients for angles between those are linearly interpolated.

- ***Free Molecular Flow:*** the sheet concerning the Free Molecular Flow regime gathers four aerodynamic coefficients: C_A, C_N, X_{CP}/L and C_m. For each of them; there are given values for five angles-of-attack 0°, 5°, 10°, 20° and 30°. Intermediate coefficients are linearly interpolated.

8. AEDB COMMENTS

8.1 UP-DATED AEDB VS PREVIOUS AEDB

A comparison of the axial force coefficients extracted from the previous database and the new calculated ones is plotted on the following figure:

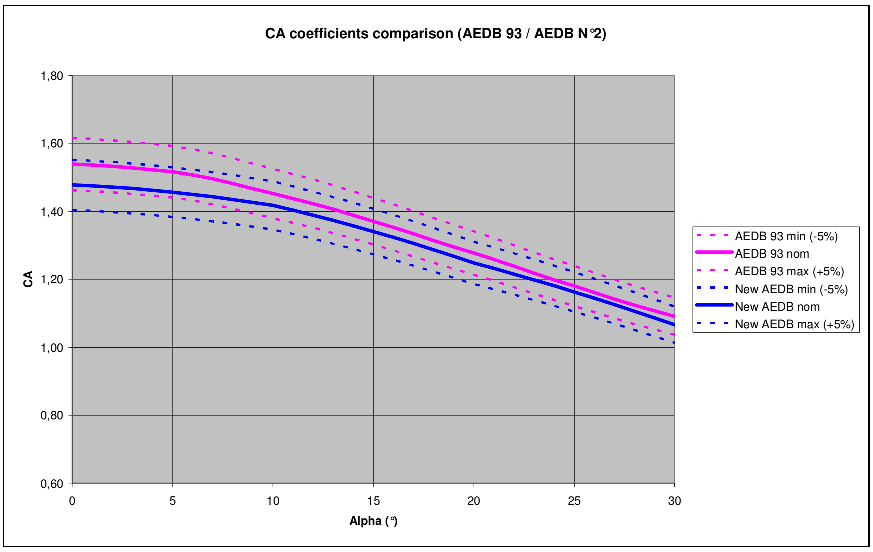

FIGURE 13 - UP-DATED DATABASE/OLD DATABASE

The present results give a lower value of about 3 to 4% at low angle-of-attack, this discrepancy decreasing when the angle-of-attack is increasing. Both angle-of-attack variation trends are similar. The same uncertainties are kept for the two databases. The two results remain within the common uncertainty range.

8.2 NEW AEDB VS OTHER COMPUTATIONS

A comparison summary of different computations and of the up-dated AEDB axial force coefficient is plotted in the following figure:

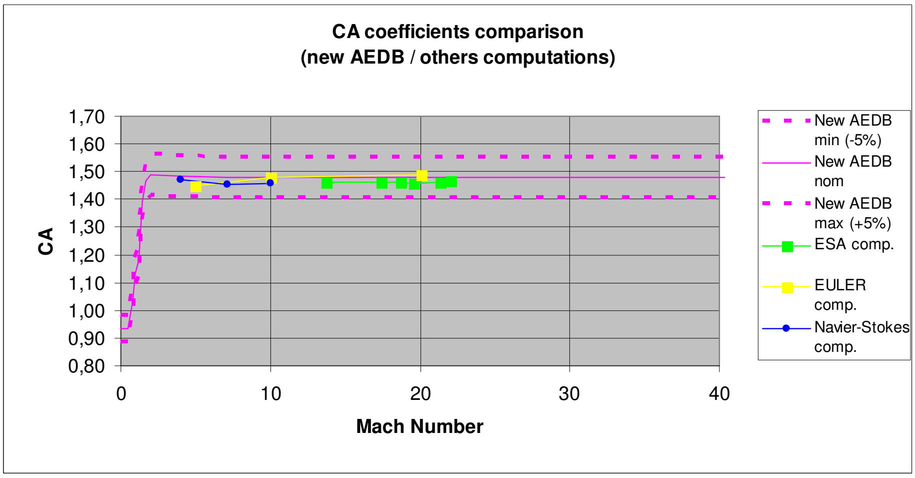

FIGURE 14 - NEW DATABASE/OTHER COMPUTATION RESULTS COMPARISON ($\alpha = 0°$)

The new nominal values calculated seem to fit correctly with others computations made with different assumptions (Code - Gas Modelisation) and coming from different sources. Moreover, keeping the previous uncertainties that we used before covers discrepancies that may be encountered while comparing values.

9. IMPACT ON TRAJECTORY

The up-dated aerodynamic coefficients are used in the BL43 6 DoF analysis tool. This code estimates the physical conditions and the flight mechanics parameters encountered by the probe along its trajectory. Entry Interface Point (EIP) is assumed at 1 270 km altitude.

Assuming the MCI characteristics of the entry module described in section 3, three entry cases corresponding to one nominal case and two worst cases (minimum and maximum conditions) covering all the possible situations Huygens can meet, have been considered:

- V_{entry} = 6 040 m/s,
- no wind is considered,
- entry relative Flight Path Angle: - 68°, - 65°, - 62°,
- initial perturbation angle: $\tau = 2°$,
- Poinsot cone angle: $\varepsilon = 2.5°$,
- initial spin rate: $p_0 = 7.4$ rpm,
- the axial force coefficient: C_A nominal, C_A - 5%, C_A + 5%,
- the Yelle density of Titan's atmosphere: nominal density, lower density, upper density.

These three cases are gathered this way:

- minimal case: - 68°, C_A minimum, $\rho_{min,}$
- nominal case: - 65°, C_A nominal, $\rho_{mon,}$
- maximal case: - 62°, C_A maximal, $\rho_{max.}$

We compare in the next pictures the conditions seen by Huygens at the Pilot Device Deployment (PDD) with the previous AEDB and the new AEDB. We also add three key parameters that are the total angle-of-attack, the Mach number and the axial acceleration.

First of all, we observe that in each case the results given by both AEDB are very similar. Lowering the axial force coefficient by about 4% does not change fundamentally the EM angle-of-attack time history during entry. Regarding the deceleration curves, the highest values reach - 152 $m.s^{-2}$ in the minimum case.

Then, in all cases, the conditions at PDD remain in the acceptable range for a correct deployment of the parachute. However, we can observe that while the dynamic pressure and the angle-of-attack at PDD are not affected by the AEDB modification, the Mach number is slightly shifted to lower values.

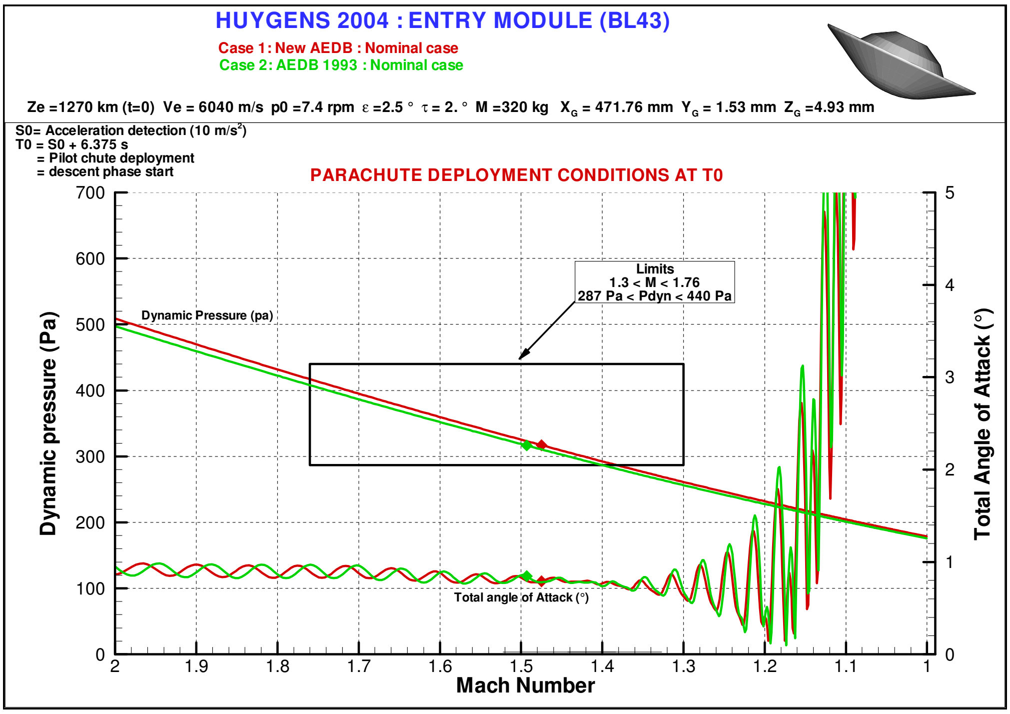

FIGURE 15 - γE = - 65° YELLE NOMINAL DENSITY: PDD CONDITIONS

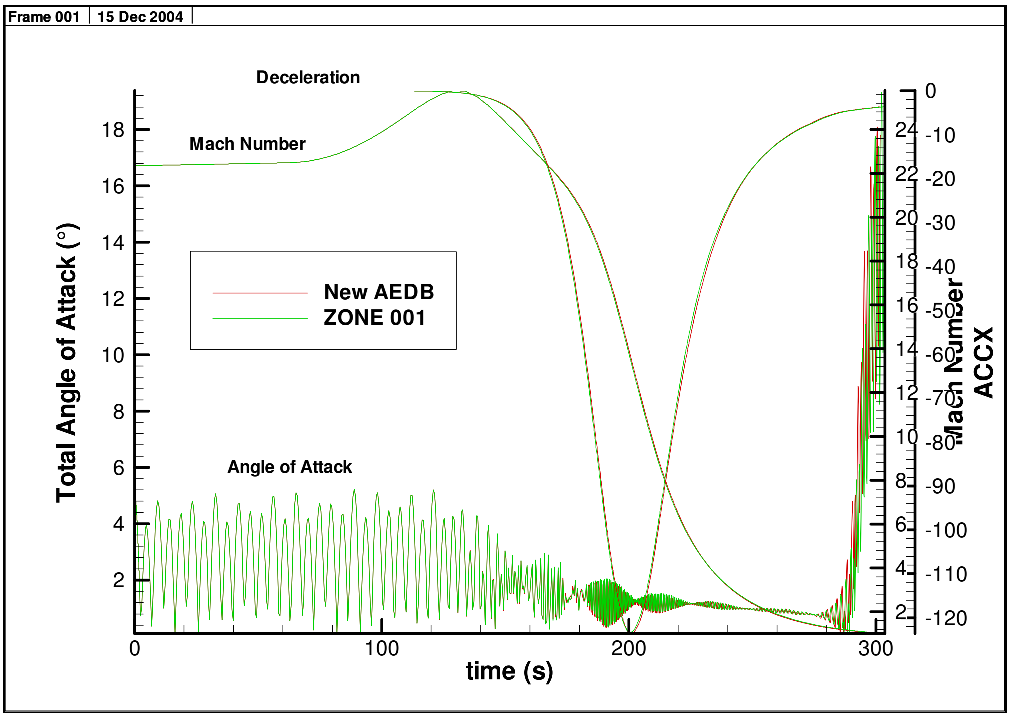

FIGURE 16 - γE = - 65° YELLE NOMINAL DENSITY: FLIGHT MECHANICS PARAMETERS

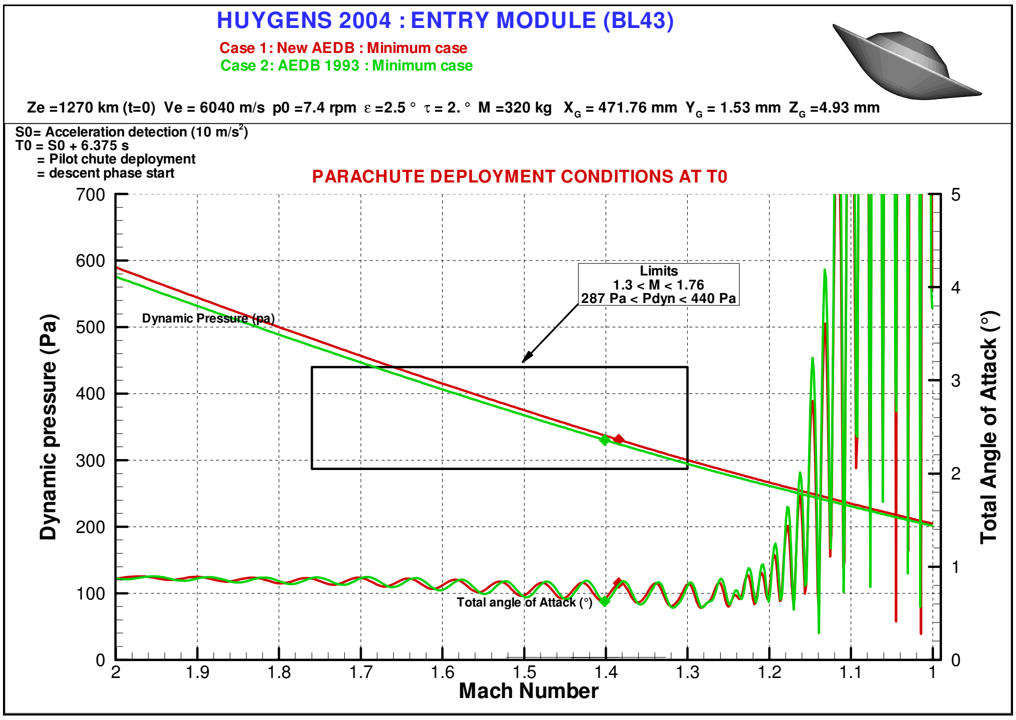

FIGURE 17 - γE = - 68° YELLE MINIMUM DENSITY: PDD CONDITIONS

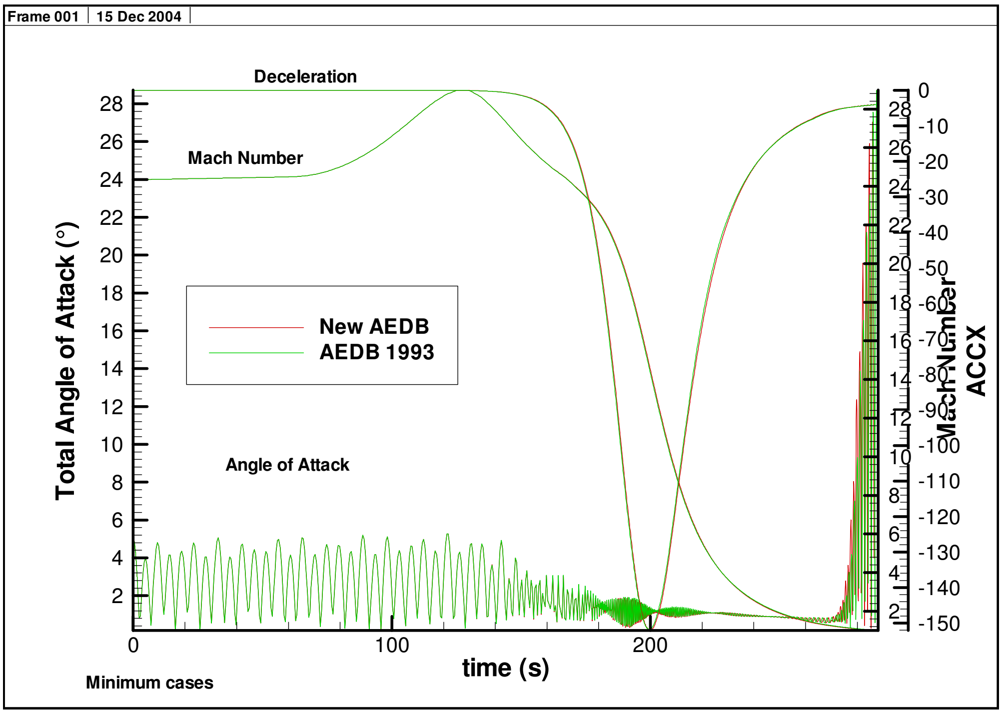

FIGURE 18 - γE = - 68° YELLE MINIMUM DENSITY: FLIGHT MECHANICS PARAMETERS

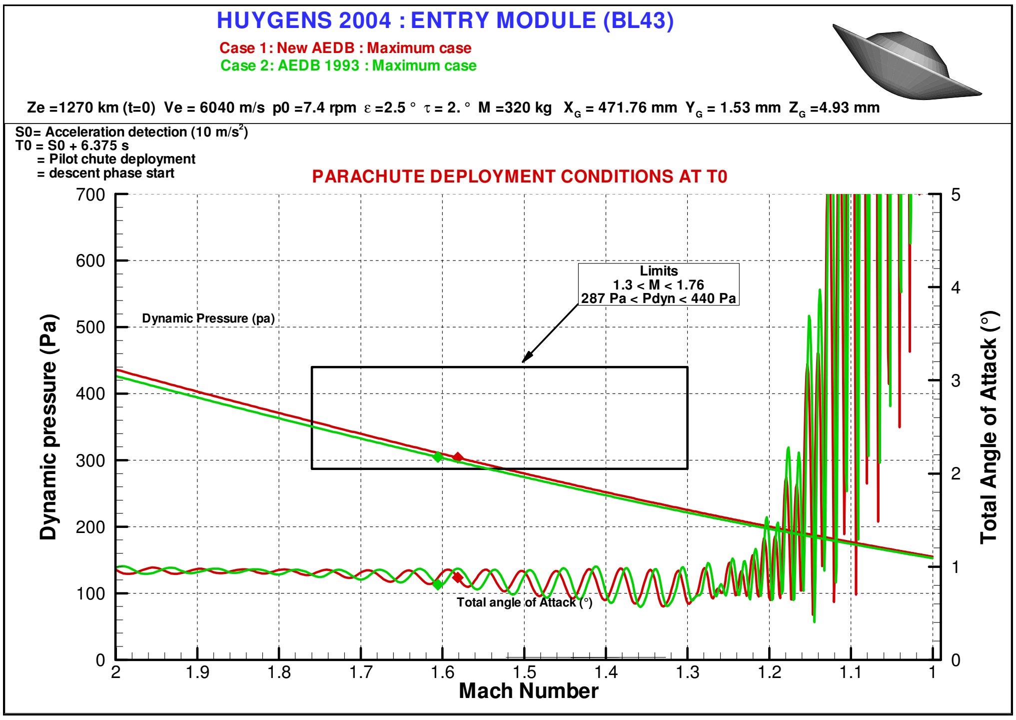

FIGURE 19 - γE = - 62° YELLE MAXIMUM DENSITY: PDD CONDITIONS

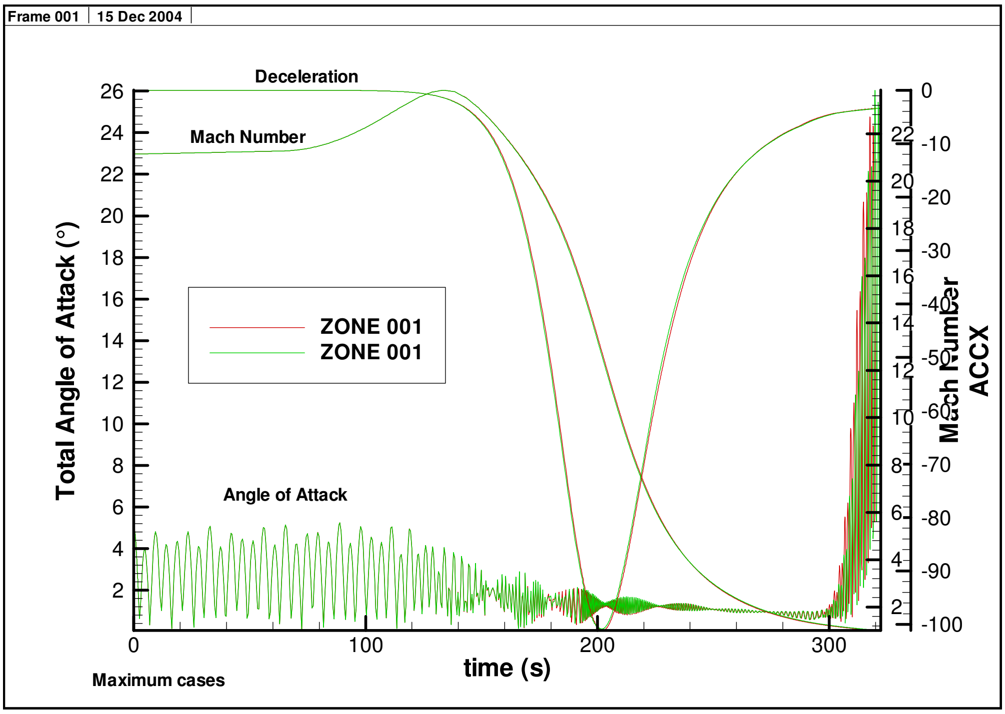

FIGURE 20 - γE = - 62° YELLE MAXIMUM DENSITY: FLIGHT MECHANICS PARAMETERS

10. CONCLUSION

The EM AEDB has been modified according to the Delta-FAR recommendations. The FFA WTT data at M = 7.15 have been removed since they were believed to be not sufficiently reliable. But for time and cost reasons, no WTT campaign was performed in order to provide with up-dated aerodynamic coefficients at M = 7.15, and CFD mean was used to address this issue. A very limited set of computations (Navier-Stokes code) was performed: M = 4, $\alpha = 0°/10°$ and M = 7.15, $\alpha = 0°/10°/20°/30°$ in FFA WT conditions and a M = 10, $\alpha = 0°$ case for verification. Only perfect gas $\gamma = 1.4$ cases were computed by EADS-ST. ESA provided some complementary results including reactive gas effects.

CFD analysis indicates that axial coefficient was questionable and only this coefficient was corrected in the EM AEDB by reducing its nominal value by approximatively 4% (at $\alpha = 0°$, CD is reduced from 1.54 down to 1.48). This nominal value is then kept constant for Mach numbers above M = 7.15. This assumption is not in contradiction with the ESA reactive gas computations results. C_N and C_m coefficients may be affected by real gas effects, but this has not been accounted for in the present up-dating, since the current values are believed to be conservative (less statically stable EM) and applicable for design. A review of rarefaction effect has been performed. DSMC computations were performed in 1992 and used to correct the C_m pitching moment coefficient for Knudsen numbers ranging between 10^{-3} and 10. Some discrepancies were found between Bridging Function and DSMC results for the C_A axial coefficients, but no correction was applied to that parameter, since no impact on the global deceleration profile was expected.

The up-dated AEDB is then assessed in terms of flight mechanics. The impact on the EM behaviour during entry is negligible. The dynamic pressure and the angle-of-attack at PDD instant are also weakly affected while the Mach number at PDD tends to be slightly lower. All these parameters remain in the EM design range.

The main purpose of the up-dated AEDB is related to the design aspect. For prediction purposes, it is necessary to improve several issues:

- drag force coefficient in transitional regime, to which past DSMC results indicated possible discrepancies. This may have an impact on the analysis of the accurate accelerometers measurements as installed in the HASI instrument. Complementary DSMC computations would be useful to that respect.

- forces and moments coefficients at high hypersonic regime. More exhaustive computations with reactive gas assumption would be useful. However, since a strong uncertainty is associated to this kind of results because of the lack of reliable experimental data, mesh refinement and code cross-checking tasks are strongly required. The European ARD flight may be used as a preceeding verification of the CFD code reactive gas capabilities. More ambitious would be to plan WTT campaign (forces and moments) in high enthalpy facilities like F4 or even HEG.

APPENDIX 1

NAVIER-STOKES CALCULATIONS MESH

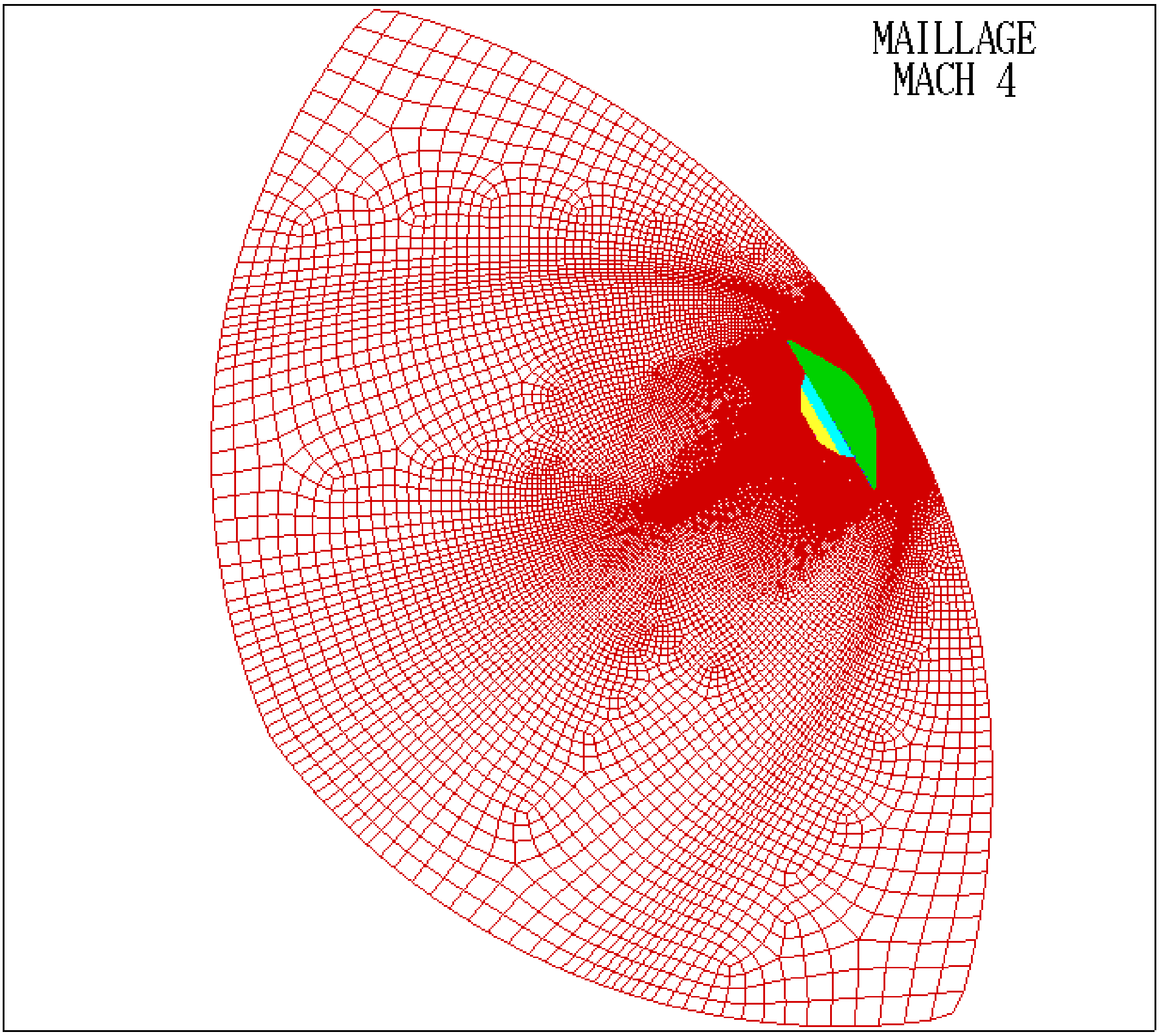

COMPUTATION DOMAIN

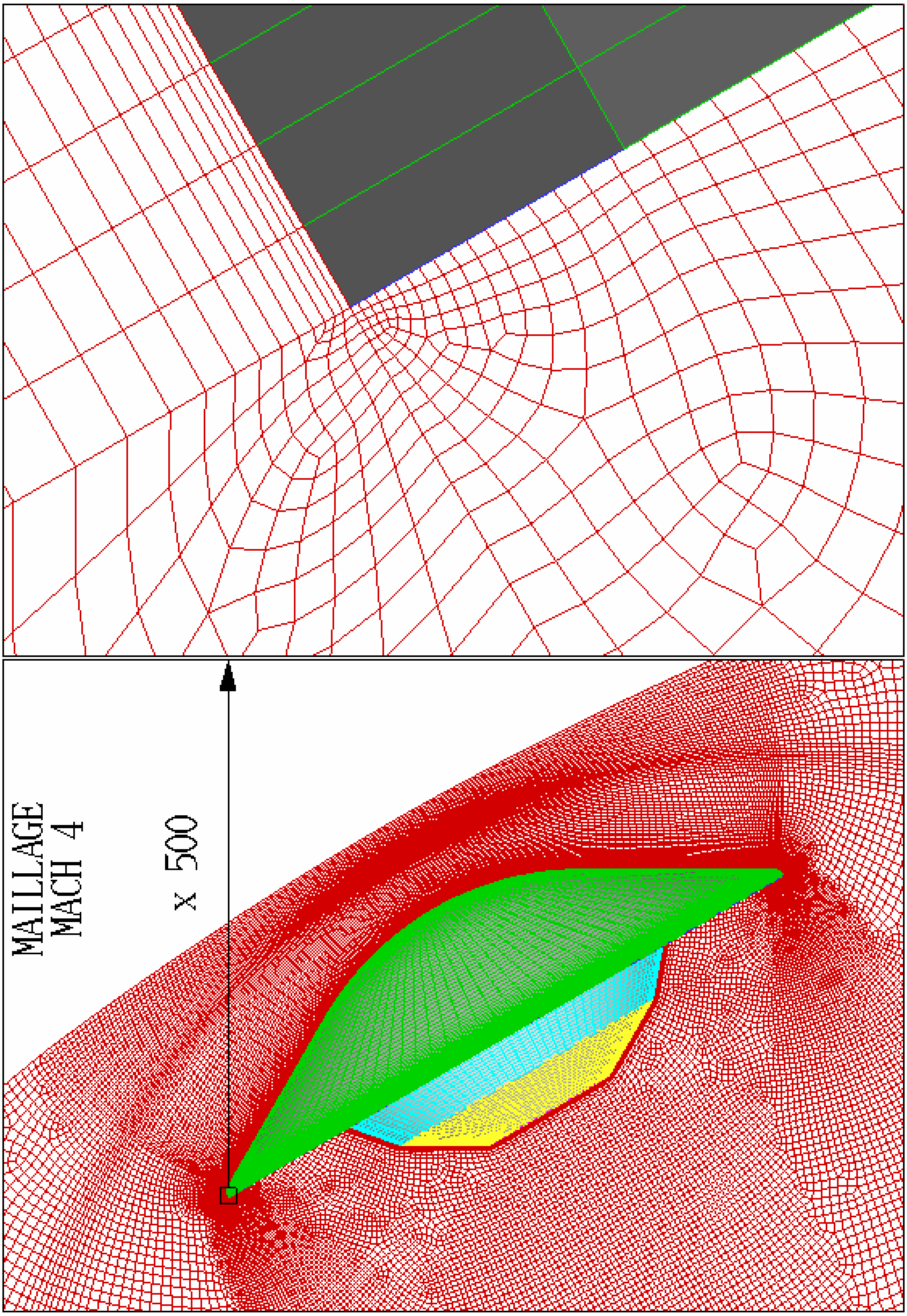

MESH DETAILS

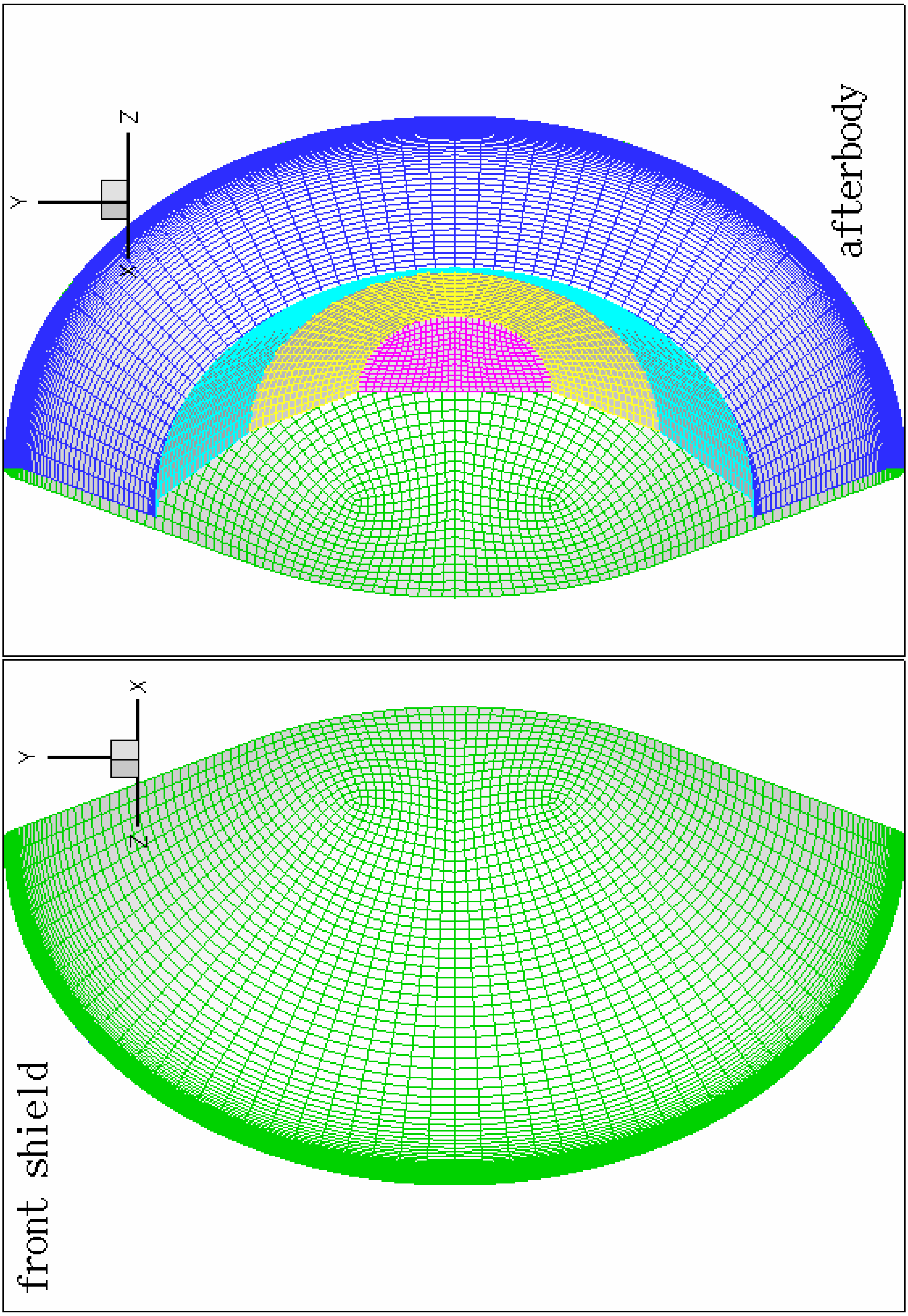

SURFACE GRIDS

APPENDIX 2

NAVIER-STOKES PRESSURE COEFFICIENT FIELD RESULTS
FOR MACH NUMBER = 4 AND 7.15

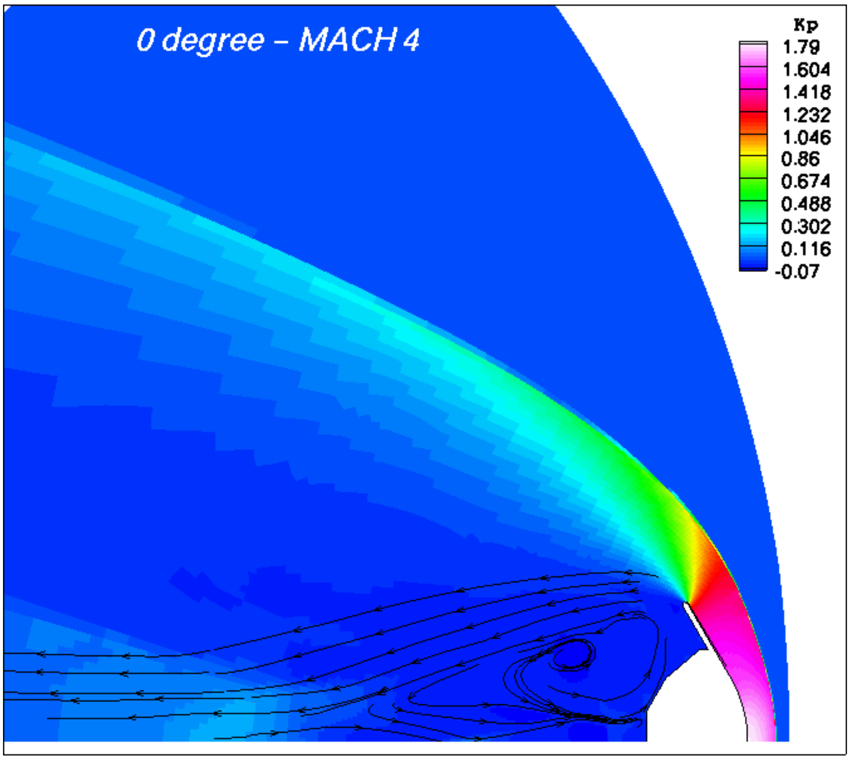

WAKE STRUCTURE AT MACH 4, α = 0°

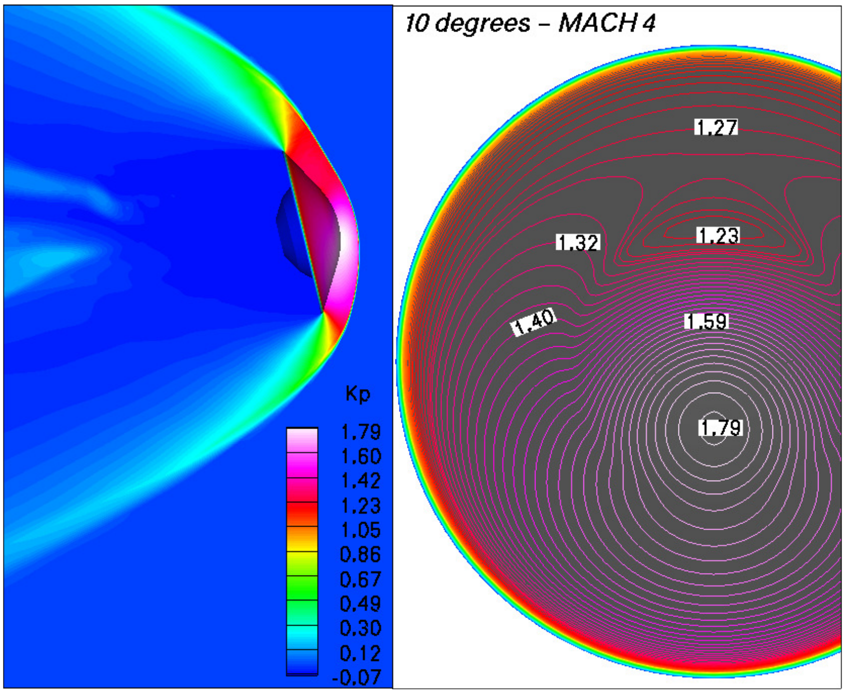

SURFACE PRESSURE COEFFICIENTS DISTRIBUTION AT MACH 4, α = 10°

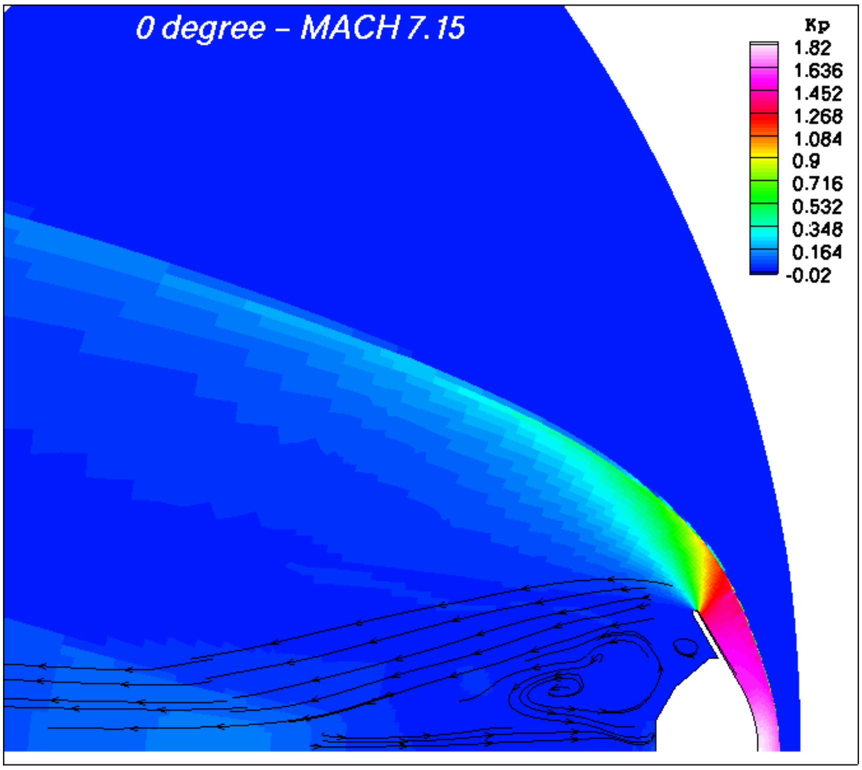

WAKE STRUCTURE AT MACH 7.15, $\alpha = 0°$

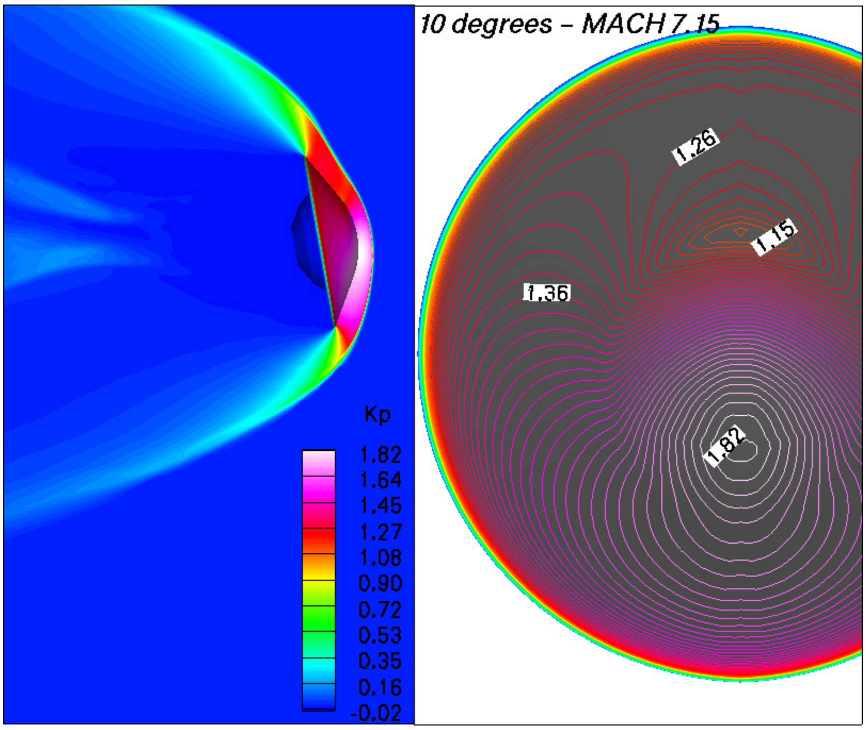

SURFACE PRESSURE COEFFICIENT DISTRIBUTION AT MACH 7.15, $\alpha = 10°$

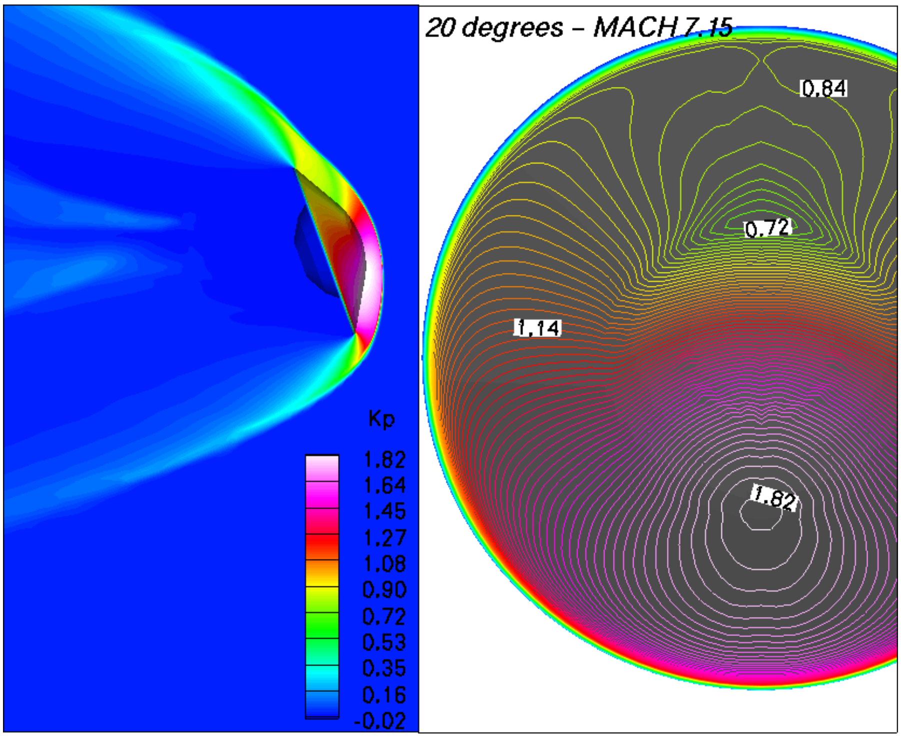

SURFACE PRESSURE COEFFICIENT DISTRIBUTION AT MACH 7.15, α = 20°

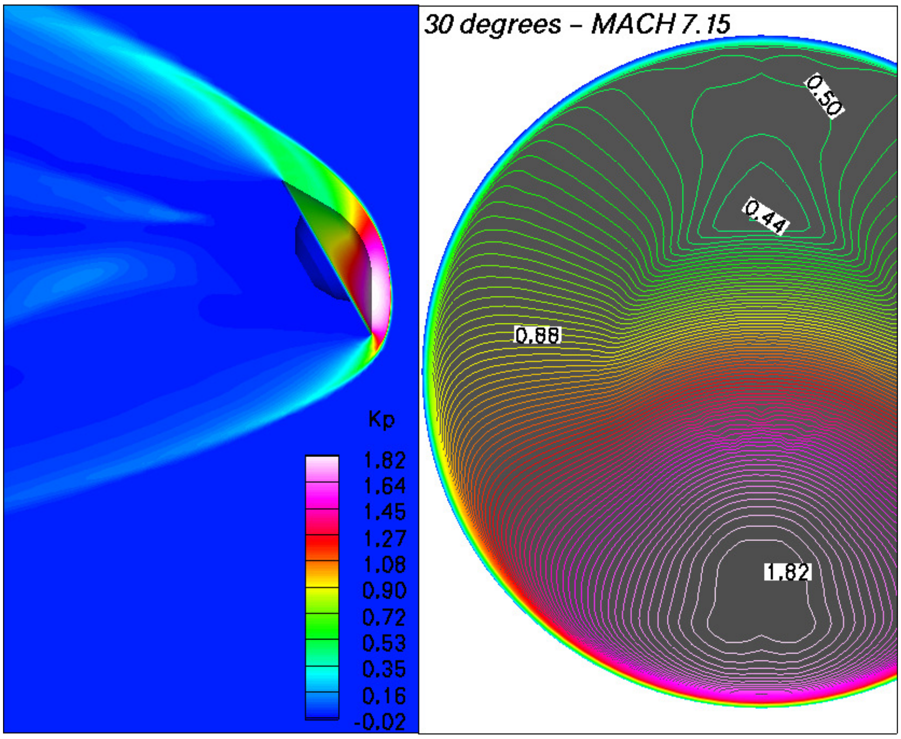

SURFACE PRESSURE COEFFICIENT DISTRIBUTION AT MACH 7.15, α = 30°

APPENDIX 3

NAVIER-STOKES MACH NUMBER FIELD
FOR MACH NUMBER = 4 AND 7.15

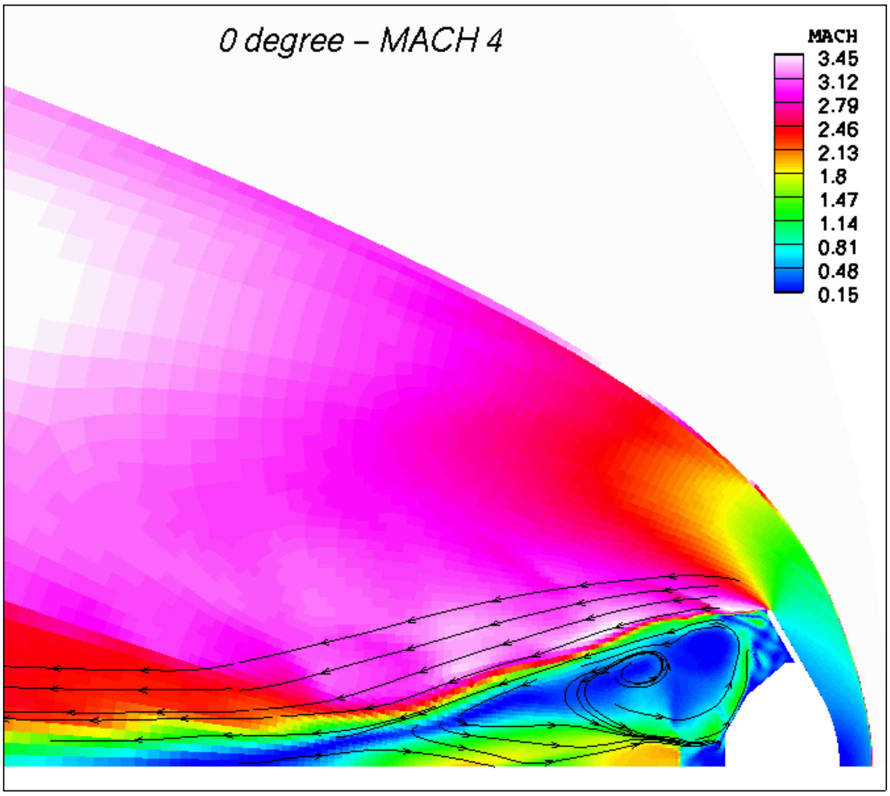

WAKE STRUCTURES AT MACH 4, α = 0°

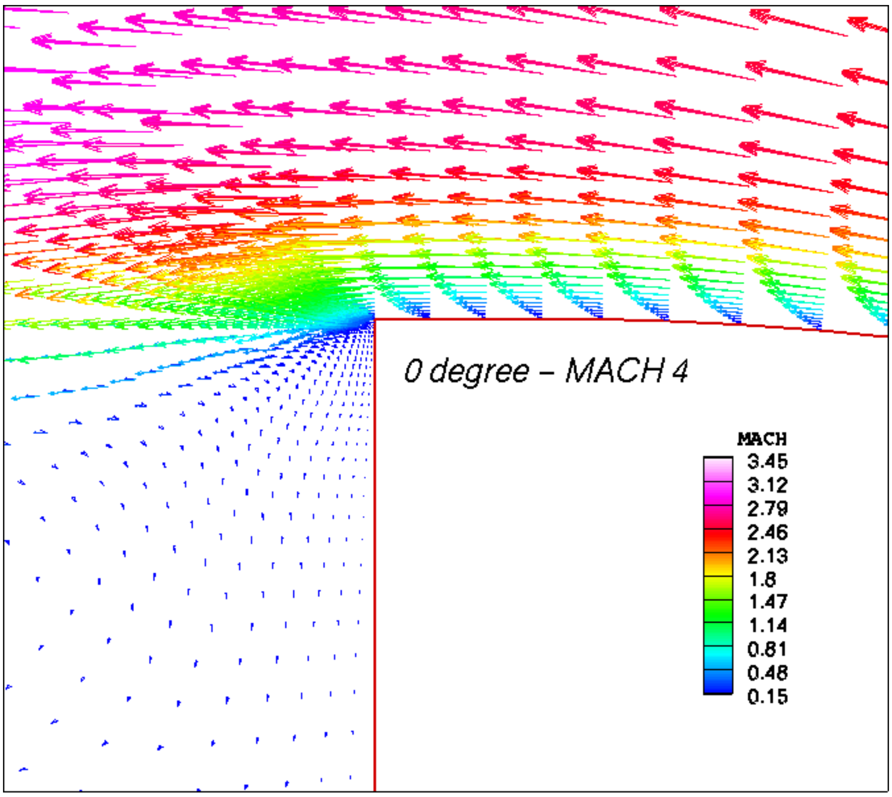

FLOW DETAILS AT SHOULDER SEPARATION AT MACH 4, α = 0°

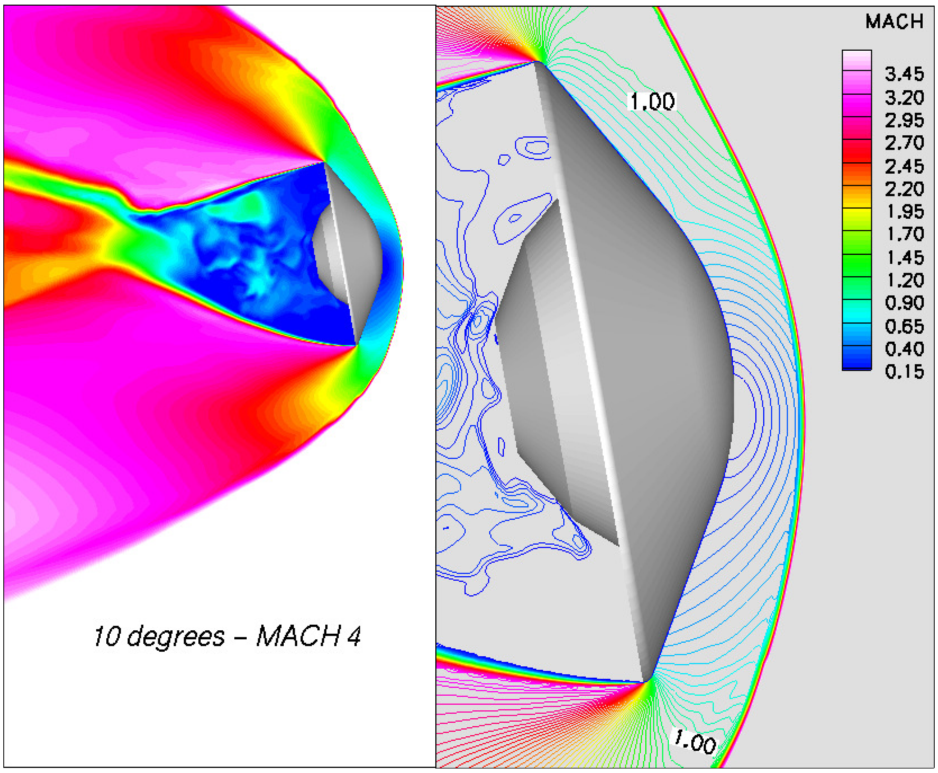

MACH 4.0 $\alpha = 10°$: LOCAL MACH NUMBER DISTRIBUTION

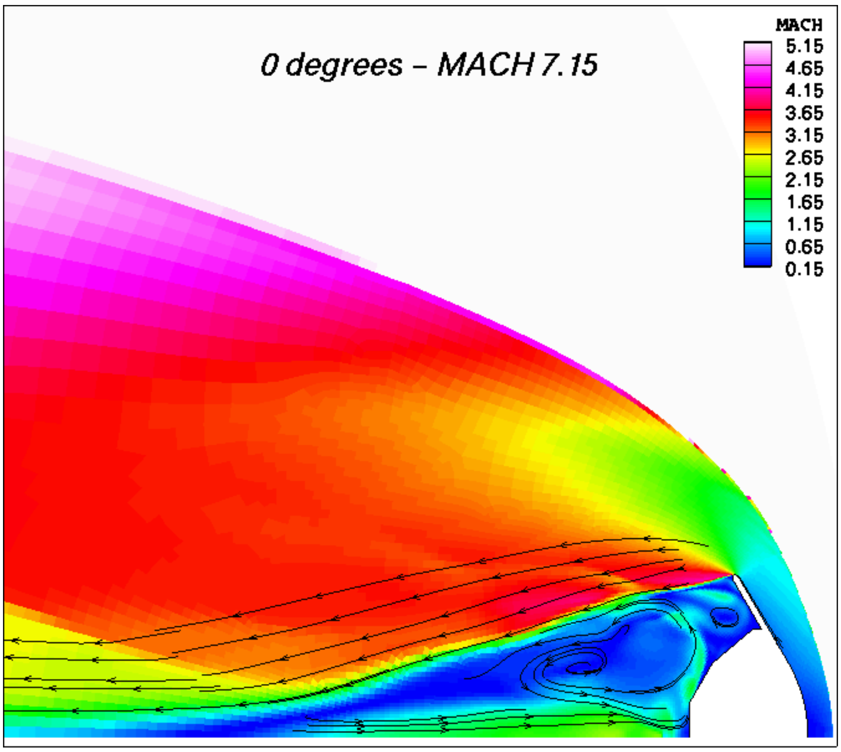

WAKE STRUCTURES AT MACH 7.15, $\alpha = 0°$

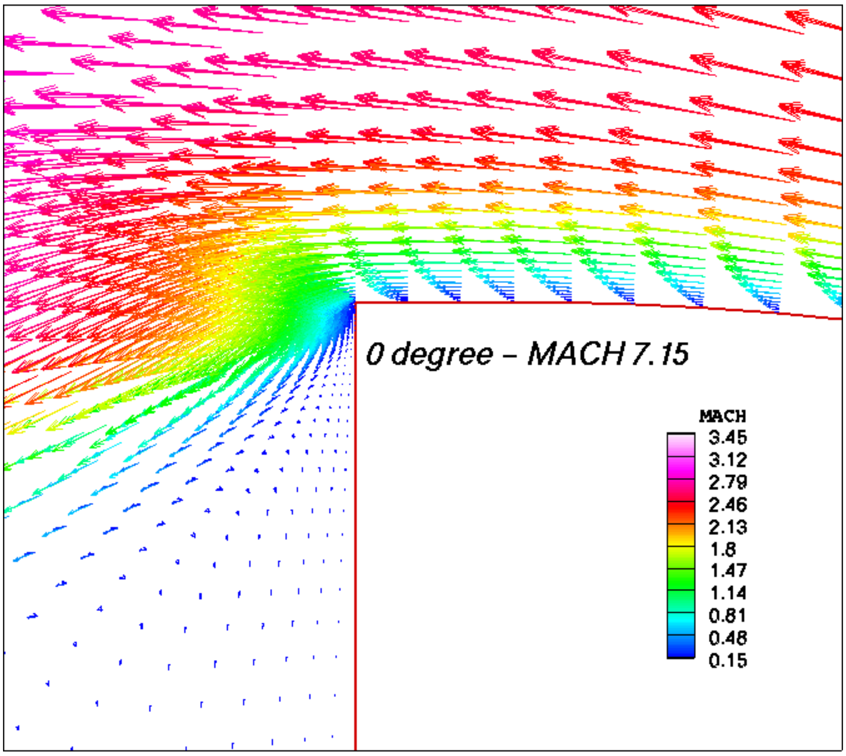

FLOW DETAILS AT SHOULDER SEPARATION AT MACH 7.15, α = 0°

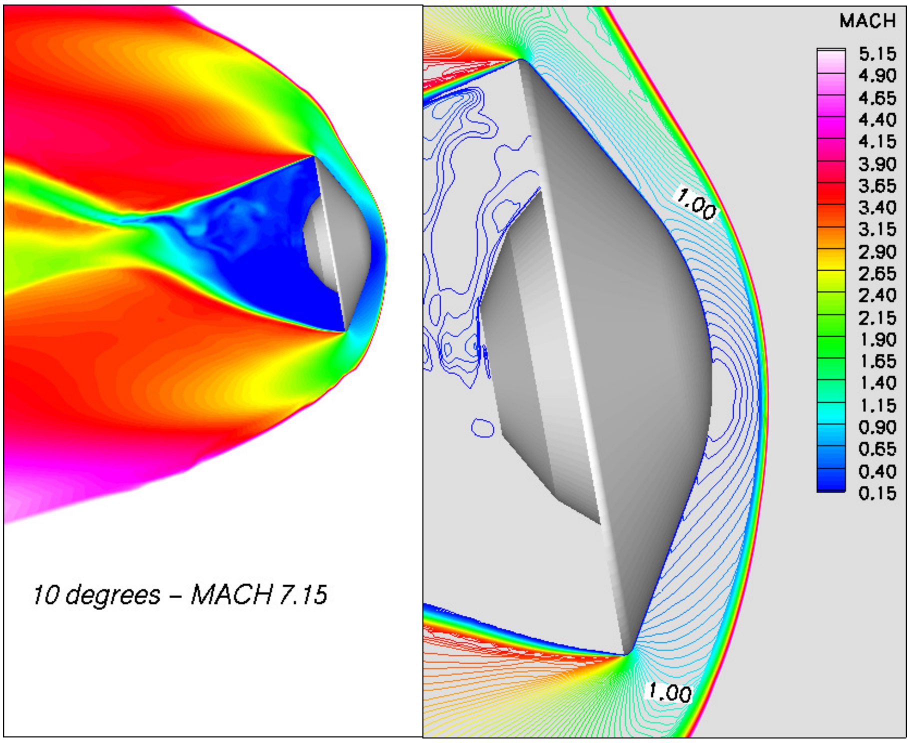

MACH 7.15 α = 10° : LOCAL MACH NUMBER DISTRIBUTION

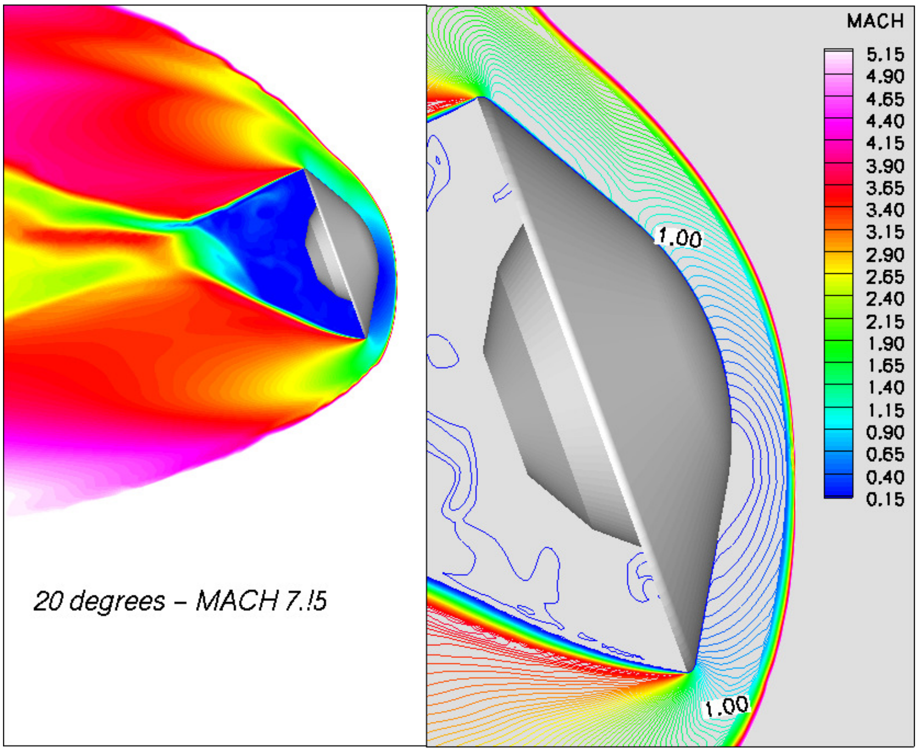

MACH 7.15 α = 20° : LOCAL MACH NUMBER DISTRIBUTION

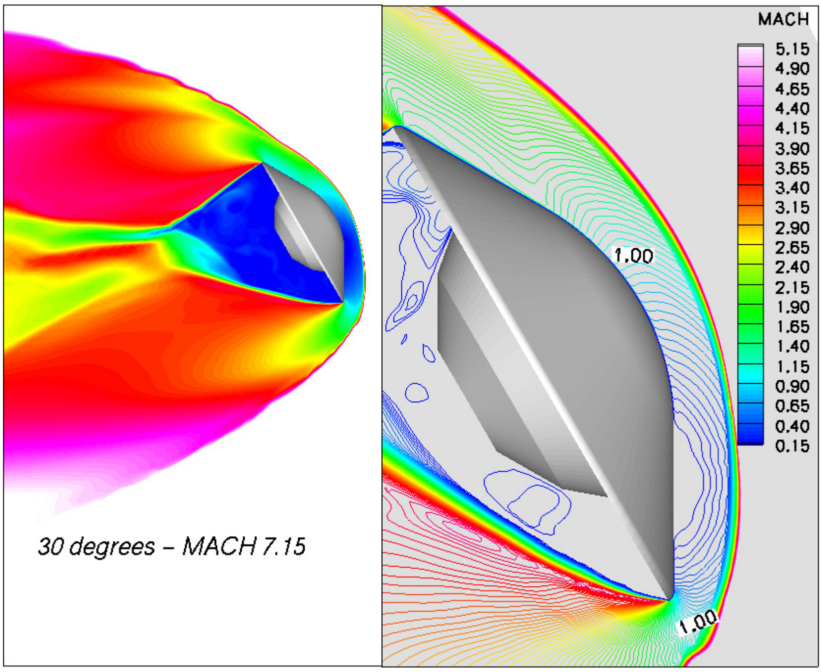

MACH 7.15 α = 30° : LOCAL MACH NUMBER DISTRIBUTION

APPENDIX 4

HUYGENS EM UP-DATED AEDB

YGENS
TRY MODULE

Axial Force Coefficient
CA

Reference length (diameter) D (m) 2,7
Reference surface Sref (m²) 5,73

	MACH												
	0	0,5	0,8	1	1,19	1,42	1,71	2,03	4	7,15	10	30	99
0	0,9349	0,9349	1,0322	1,1338	1,1827	1,3941	1,4646	1,489	1,4834	1,4780	1,4780	1,4780	1,4780
1	0,9385	0,9385	1,0305	1,134	1,1844	1,3972	1,4673	1,4906	1,4809	1,4719	1,4719	1,4719	1,4719
2	0,9398	0,9398	1,0286	1,1355	1,1874	1,4034	1,4699	1,4918	1,4775	1,4658	1,4658	1,4658	1,4658
3	0,9393	0,9393	1,0266	1,1378	1,1908	1,4082	1,4714	1,4923	1,4739	1,4598	1,4598	1,4598	1,4598
4	0,9346	0,9346	1,0259	1,1404	1,1936	1,4082	1,4722	1,4924	1,4701	1,4537	1,4537	1,4537	1,4537
5	0,9269	0,9269	1,0262	1,1433	1,1947	1,4061	1,4734	1,4925	1,4654	1,4476	1,4476	1,4476	1,4476
6	0,9213	0,9213	1,0258	1,1444	1,1942	1,4063	1,4748	1,4926	1,4597	1,4415	1,4415	1,4415	1,4415
7	0,9182	0,9182	1,0249	1,1432	1,194	1,4095	1,4751	1,4919	1,4525	1,4355	1,4355	1,4355	1,4355
8	0,9157	0,9157	1,0243	1,1432	1,1951	1,4137	1,4747	1,4906	1,4444	1,4294	1,4294	1,4294	1,4294
9	0,9139	0,9139	1,0241	1,1453	1,1971	1,4172	1,4744	1,4888	1,4355	1,4233	1,4233	1,4233	1,4233
10	0,9119	0,9119	1,0237	1,1461	1,199	1,4202	1,474	1,4868	1,4251	1,4172	1,4172	1,4172	1,4172
11	0,9098	0,9098	1,0191	1,1484	1,2019	1,4232	1,4732	1,4843	1,4131	1,4003	1,4003	1,4003	1,4003
12	0,9079	0,9079	1,0125	1,1539	1,206	1,4259	1,4719	1,4816	1,3997	1,3834	1,3834	1,3834	1,3834
13	0,9054	0,9054	1,0094	1,158	1,2083	1,4277	1,4696	1,4781	1,3851	1,3665	1,3665	1,3665	1,3665
14	0,9027	0,9027	1,0083	1,1593	1,2083	1,4285	1,4659	1,4733	1,3697	1,3496	1,3496	1,3496	1,3496
15	0,8994	0,8994	1,0059	1,162	1,2091	1,4283	1,4615	1,4674	1,3541	1,3327	1,3327	1,3327	1,3327
16	0,8951	0,8951	1,0032	1,1679	1,2119	1,4274	1,4563	1,4607	1,3378	1,3158	1,3158	1,3158	1,3158
17	0,8901	0,8901	1,0009	1,1713	1,2131	1,4256	1,4505	1,453	1,3207	1,2989	1,2989	1,2989	1,2989
18	0,8845	0,8845	0,9973	1,1732	1,2103	1,4227	1,4448	1,4443	1,3029	1,2819	1,2819	1,2819	1,2819
19	0,8788	0,8788	0,9948	1,1795	1,2064	1,419	1,4387	1,4345	1,2844	1,2650	1,2650	1,2650	1,2650
20	0,8729	0,8729	0,9908	1,1872	1,2024	1,4148	1,4316	1,4237	1,2664	1,2481	1,2481	1,2481	1,2481
21	0,8667	0,8667	0,9825	1,1914	1,1968	1,4098	1,4243	1,4118	1,2487	1,2299	1,2299	1,2299	1,2299
22	0,859	0,859	0,9737	1,1912	1,1905	1,4039	1,4172	1,3988	1,2303	1,2118	1,2118	1,2118	1,2118
23	0,8507	0,8507	0,9647	1,1885	1,1852	1,3975	1,4092	1,385	1,2117	1,1936	1,1936	1,1936	1,1936
24	0,8424	0,8424	0,9541	1,1869	1,1801	1,3905	1,3993	1,3701	1,1937	1,1754	1,1754	1,1754	1,1754
25	0,8338	0,8338	0,9431	1,1868	1,1739	1,383	1,388	1,3542	1,1758	1,1572	1,1572	1,1572	1,1572
26	0,8252	0,8252	0,9319	1,185	1,1667	1,3752	1,3757	1,3375	1,1575	1,1391	1,1391	1,1391	1,1391
27	0,8161	0,8161	0,9196	1,1813	1,1583	1,3672	1,3621	1,3201	1,1391	1,1209	1,1209	1,1209	1,1209
28	0,8052	0,8052	0,907	1,1772	1,148	1,359	1,3473	1,3019	1,1211	1,1027	1,1027	1,1027	1,1027
30	0,7722	0,7722	0,874	1,1442	1,115	1,326	1,3143	1,2689	1,0881	1,0663	1,0663	1,0663	1,0663
40	0,5882	0,5882	0,69	0,9602	0,931	1,142	1,1303	1,0849	0,9041	0,8823	0,8823	0,8823	0,8823
50	0,3942	0,3942	0,496	0,7662	0,737	0,948	0,9363	0,8909	0,7101	0,6883	0,6883	0,6883	0,6883
60	0,2022	0,2022	0,304	0,5742	0,545	0,756	0,7443	0,6989	0,5181	0,4963	0,4963	0,4963	0,4963
70	0,0202	0,0202	0,122	0,3922	0,363	0,574	0,5623	0,5169	0,3361	0,3143	0,3143	0,3143	0,3143
80	-0,1478	-0,1478	-0,046	0,2242	0,195	0,406	0,3943	0,3489	0,1681	0,1463	0,1463	0,1463	0,1463
90	-0,3068	-0,3068	-0,205	0,0652	0,036	0,247	0,2353	0,1899	0,0091	-0,0127	-0,0127	-0,0127	-0,0127

YGENS
TRY MODULE

Normal Force Coefficient
CN

Reference length (diameter) D (m) 2,7
Reference surface Sref (m²) 5,73

	MACH												
	0	0,5	0,8	1	1,19	1,42	1,71	2,03	4	7,15	10	30	99
0	0	0	0	0	0	0	0	0	0	0	0	0	0
1	0,0034	0,0034	0,0032	0,0027	0,0025	0,0027	0,0031	0,0034	0,0042	0,0046	0,0046	0,0046	0,0046
2	0,0069	0,0069	0,0063	0,0055	0,005	0,0055	0,0065	0,007	0,0085	0,0093	0,0093	0,0093	0,0093
3	0,0105	0,0105	0,0095	0,0085	0,0075	0,0086	0,0102	0,0109	0,0128	0,0141	0,0141	0,0141	0,0141
4	0,014	0,014	0,0129	0,0116	0,0103	0,0121	0,0141	0,0149	0,0172	0,019	0,019	0,019	0,019
5	0,0176	0,0176	0,0168	0,0148	0,0134	0,0158	0,0181	0,0191	0,0216	0,024	0,024	0,024	0,024
6	0,0212	0,0212	0,021	0,0184	0,0169	0,0197	0,0221	0,0233	0,0262	0,0296	0,0296	0,0296	0,0296
7	0,0248	0,0248	0,0251	0,0224	0,0207	0,0236	0,0261	0,0275	0,0309	0,0359	0,0359	0,0359	0,0359
8	0,0287	0,0287	0,0292	0,0267	0,0246	0,0276	0,0301	0,0316	0,0357	0,0426	0,0426	0,0426	0,0426
9	0,0327	0,0327	0,0335	0,031	0,0286	0,0315	0,034	0,0357	0,0407	0,0495	0,0495	0,0495	0,0495
10	0,0367	0,0367	0,0379	0,0351	0,0325	0,0355	0,038	0,0398	0,046	0,0565	0,0565	0,0565	0,0565
11	0,0406	0,0406	0,0424	0,0392	0,0364	0,0394	0,0418	0,0438	0,0516	0,0633	0,0633	0,0633	0,0633
12	0,0448	0,0448	0,0471	0,0435	0,0402	0,0433	0,0457	0,0478	0,0574	0,0698	0,0698	0,0698	0,0698
13	0,049	0,049	0,0518	0,0478	0,0439	0,0471	0,0496	0,0518	0,0634	0,0767	0,0767	0,0767	0,0767
14	0,0533	0,0533	0,0561	0,0519	0,0476	0,0509	0,0534	0,0558	0,0696	0,0838	0,0838	0,0838	0,0838
15	0,0576	0,0576	0,0608	0,0561	0,0513	0,0546	0,0572	0,0599	0,0756	0,0909	0,0909	0,0909	0,0909
16	0,0618	0,0618	0,0656	0,0602	0,055	0,0582	0,061	0,064	0,0816	0,0979	0,0979	0,0979	0,0979
17	0,0661	0,0661	0,0701	0,0642	0,0586	0,0618	0,0648	0,0681	0,0875	0,1047	0,1047	0,1047	0,1047
18	0,0704	0,0704	0,0743	0,0682	0,0621	0,0653	0,0686	0,0722	0,0936	0,1114	0,1114	0,1114	0,1114
19	0,0747	0,0747	0,0785	0,0721	0,0657	0,0689	0,0724	0,0765	0,0999	0,1178	0,1178	0,1178	0,1178
20	0,0787	0,0787	0,0827	0,076	0,0691	0,0726	0,0762	0,0807	0,1059	0,1236	0,1236	0,1236	0,1236
21	0,0826	0,0826	0,0868	0,08	0,0726	0,0761	0,08	0,0849	0,1116	0,1295	0,1295	0,1295	0,1295
22	0,0863	0,0863	0,0907	0,0837	0,076	0,0797	0,0838	0,0892	0,1172	0,1359	0,1359	0,1359	0,1359
23	0,0902	0,0902	0,0949	0,0874	0,0794	0,0832	0,0877	0,0936	0,1228	0,142	0,142	0,142	0,142
24	0,0939	0,0939	0,0991	0,0912	0,0828	0,0868	0,0917	0,0981	0,1282	0,1478	0,1478	0,1478	0,1478
25	0,0974	0,0974	0,103	0,095	0,0861	0,0903	0,0957	0,1028	0,1334	0,1532	0,1532	0,1532	0,1532
26	0,1009	0,1009	0,1069	0,0986	0,0894	0,0939	0,0997	0,1075	0,1384	0,1582	0,1582	0,1582	0,1582
27	0,1044	0,1044	0,111	0,1024	0,0927	0,0975	0,1039	0,1125	0,1431	0,1628	0,1628	0,1628	0,1628
28	0,1081	0,1081	0,1153	0,1062	0,0962	0,1013	0,1082	0,1177	0,1475	0,1669	0,1669	0,1669	0,1669
30	0,1161	0,1161	0,1233	0,1142	0,1042	0,1093	0,1162	0,1257	0,1555	0,1749	0,1749	0,1749	0,1749
40	0,1411	0,1411	0,1483	0,1392	0,1292	0,1343	0,1412	0,1507	0,1805	0,1999	0,1999	0,1999	0,1999
50	0,1411	0,1411	0,1483	0,1392	0,1292	0,1343	0,1412	0,1507	0,1805	0,1999	0,1999	0,1999	0,1999
60	0,1211	0,1211	0,1283	0,1192	0,1092	0,1143	0,1212	0,1307	0,1605	0,1799	0,1799	0,1799	0,1799
70	0,0881	0,0881	0,0953	0,0862	0,0762	0,0813	0,0882	0,0977	0,1275	0,1469	0,1469	0,1469	0,1469
80	0,0501	0,0501	0,0573	0,0482	0,0382	0,0433	0,0502	0,0597	0,0895	0,1089	0,1089	0,1089	0,1089
90	0,0151	0,0151	0,0223	0,0132	0,0032	0,0083	0,0152	0,0247	0,0545	0,0739	0,0739	0,0739	0,0739

YGENS
TRY MODULE

Pitching Moment Coefficient
Cm at 0.265*D

Reference length (diameter)	D (m)	2,7
Reference surface	Sref (m²)	5,73

	MACH												
	0	0,5	0,8	1	1,19	1,42	1,71	2,03	4	7,15	10	30	99
0	0	0	0	0	0	0	0	0	0	0	0	0	0
1	-0,0027	-0,0027	-0,0028	-0,0031	-0,0032	-0,0031	-0,0028	-0,0027	-0,0021	-0,002	-0,002	-0,002	-0,002
2	-0,0053	-0,0053	-0,0057	-0,0061	-0,0062	-0,0059	-0,0052	-0,0051	-0,0042	-0,0041	-0,0041	-0,0041	-0,0041
3	-0,0079	-0,0079	-0,0086	-0,0088	-0,0089	-0,0082	-0,0071	-0,0071	-0,0061	-0,0061	-0,0061	-0,0061	-0,0061
4	-0,0105	-0,0105	-0,0113	-0,0114	-0,0111	-0,0099	-0,0086	-0,0088	-0,0079	-0,0082	-0,0082	-0,0082	-0,0082
5	-0,013	-0,013	-0,0137	-0,0136	-0,0129	-0,0114	-0,0101	-0,0105	-0,0097	-0,0103	-0,0103	-0,0103	-0,0103
6	-0,0153	-0,0153	-0,016	-0,0156	-0,0144	-0,0127	-0,0116	-0,0121	-0,0116	-0,0127	-0,0127	-0,0127	-0,0127
7	-0,0177	-0,0177	-0,0182	-0,0173	-0,0157	-0,0141	-0,0132	-0,0138	-0,0135	-0,0153	-0,0153	-0,0153	-0,0153
8	-0,02	-0,02	-0,0203	-0,0188	-0,0171	-0,0155	-0,0149	-0,0156	-0,0155	-0,0183	-0,0183	-0,0183	-0,0183
9	-0,0223	-0,0223	-0,0224	-0,0205	-0,0186	-0,0169	-0,0166	-0,0174	-0,0176	-0,0214	-0,0214	-0,0214	-0,0214
10	-0,0245	-0,0245	-0,0245	-0,0223	-0,02	-0,0185	-0,0183	-0,0192	-0,0198	-0,0245	-0,0245	-0,0245	-0,0245
11	-0,0267	-0,0267	-0,0265	-0,0241	-0,0216	-0,0201	-0,0201	-0,0211	-0,0222	-0,0276	-0,0276	-0,0276	-0,0276
12	-0,0289	-0,0289	-0,0285	-0,0259	-0,0231	-0,0217	-0,0219	-0,023	-0,0248	-0,0307	-0,0307	-0,0307	-0,0307
13	-0,031	-0,031	-0,0305	-0,0276	-0,0247	-0,0234	-0,0237	-0,0249	-0,0274	-0,0339	-0,0339	-0,0339	-0,0339
14	-0,0331	-0,0331	-0,0327	-0,0294	-0,0262	-0,0251	-0,0255	-0,0267	-0,0301	-0,0373	-0,0373	-0,0373	-0,0373
15	-0,035	-0,035	-0,0348	-0,0312	-0,0278	-0,0268	-0,0273	-0,0286	-0,0329	-0,0407	-0,0407	-0,0407	-0,0407
16	-0,037	-0,037	-0,0368	-0,0329	-0,0293	-0,0285	-0,0291	-0,0305	-0,0356	-0,0441	-0,0441	-0,0441	-0,0441
17	-0,0389	-0,0389	-0,0388	-0,0347	-0,0309	-0,0302	-0,0309	-0,0324	-0,0383	-0,0475	-0,0475	-0,0475	-0,0475
18	-0,0409	-0,0409	-0,0409	-0,0365	-0,0325	-0,032	-0,0327	-0,0343	-0,0412	-0,0509	-0,0509	-0,0509	-0,0509
19	-0,0428	-0,0428	-0,043	-0,0383	-0,0341	-0,0338	-0,0345	-0,0362	-0,0442	-0,0542	-0,0542	-0,0542	-0,0542
20	-0,0448	-0,0448	-0,0451	-0,0401	-0,0356	-0,0355	-0,0363	-0,0381	-0,0471	-0,0572	-0,0572	-0,0572	-0,0572
21	-0,0468	-0,0468	-0,047	-0,0419	-0,0372	-0,0373	-0,0382	-0,0401	-0,0499	-0,0602	-0,0602	-0,0602	-0,0602
22	-0,0486	-0,0486	-0,049	-0,0436	-0,0387	-0,039	-0,04	-0,042	-0,0526	-0,0634	-0,0634	-0,0634	-0,0634
23	-0,0504	-0,0504	-0,051	-0,0454	-0,0403	-0,0407	-0,0418	-0,0441	-0,0554	-0,0666	-0,0666	-0,0666	-0,0666
24	-0,0521	-0,0521	-0,0529	-0,0471	-0,0418	-0,0424	-0,0436	-0,0461	-0,058	-0,0696	-0,0696	-0,0696	-0,0696
25	-0,0539	-0,0539	-0,0547	-0,0488	-0,0434	-0,0441	-0,0454	-0,0482	-0,0606	-0,0724	-0,0724	-0,0724	-0,0724
26	-0,0557	-0,0557	-0,0565	-0,0505	-0,0449	-0,0458	-0,0472	-0,0503	-0,0632	-0,075	-0,075	-0,075	-0,075
27	-0,0574	-0,0574	-0,0584	-0,0522	-0,0464	-0,0476	-0,049	-0,0526	-0,0655	-0,0774	-0,0774	-0,0774	-0,0774
28	-0,059	-0,059	-0,0603	-0,0538	-0,048	-0,0493	-0,051	-0,0549	-0,0677	-0,0795	-0,0795	-0,0795	-0,0795
30	-0,067	-0,067	-0,0683	-0,0618	-0,056	-0,0573	-0,059	-0,0629	-0,0757	-0,0875	-0,0875	-0,0875	-0,0875
40	-0,09	-0,09	-0,0913	-0,0848	-0,079	-0,0803	-0,082	-0,0859	-0,0987	-0,1105	-0,1105	-0,1105	-0,1105
50	-0,089	-0,089	-0,0903	-0,0838	-0,078	-0,0793	-0,081	-0,0849	-0,0977	-0,1095	-0,1095	-0,1095	-0,1095
60	-0,068	-0,068	-0,0693	-0,0628	-0,057	-0,0583	-0,06	-0,0639	-0,0767	-0,0885	-0,0885	-0,0885	-0,0885
70	-0,034	-0,034	-0,0353	-0,0288	-0,023	-0,0243	-0,026	-0,0299	-0,0427	-0,0545	-0,0545	-0,0545	-0,0545
80	0,004	0,004	0,0027	0,0092	0,015	0,0137	0,012	0,0081	-0,0047	-0,0165	-0,0165	-0,0165	-0,0165
90	0,04	0,04	0,0387	0,0452	0,051	0,0497	0,048	0,0441	0,0313	0,0195	0,0195	0,0195	0,0195

'GENS

RY MODULE

Pitch Damping Coefficient

$C_{mq} + C_{m\dot{\alpha}}$°

Reference length (diameter) D (m) 2,7

Reference surface Sref (m²) 5,73

	MACH																					
	0	0,6	0,65	0,8	1	1,1	1,15	1,2	1,4	1,71	1,8	1,9	2	2,1	2,2	2,3	2,4	2,5	2,6	2,7	2,9	100
0	0,15	0,15	0,25	0,5	1	1,5	1,5	1	0,4	0,44	0,33	0,22	0,22	0,22	0,11	0	0	0	0	0	0	0
1	0,15	0,15	0,25	0,5	1	1,5	1,5	1	0,4	0	-0,08	-0,08	-0,108	-0,108	-0,162	-0,162	-0,162	-0,162	-0,108	-0,216	-0,171	-0,171
2	0,1	0,1	0,2	0,4	0,7	1,4	1,4	0,88	0,35	-0,108	-0,108	-0,108	-0,162	-0,162	-0,162	-0,162	-0,162	-0,162	-0,162	-0,216	-0,171	-0,171
3	0,1	0,1	0,2	0,4	0,7	1,4	1,4	0,88	0,35	-0,162	-0,162	-0,162	-0,162	-0,162	-0,162	-0,162	-0,162	-0,162	-0,162	-0,216	-0,171	-0,171
4	0,05	0,05	0,15	0,29	0,45	1,2	1,2	0,67	0,28	-0,162	-0,162	-0,162	-0,162	-0,162	-0,162	-0,162	-0,162	-0,162	-0,162	-0,216	-0,171	-0,171
6	0,02	0,02	0,1	0,21	0,33	1	1	0,56	0,23	-0,162	-0,162	-0,162	-0,162	-0,162	-0,162	-0,162	-0,162	-0,162	-0,162	-0,216	-0,171	-0,171
8	0	0	0,05	0,14	0,2	0,7	0,7	0,42	0,17	-0,162	-0,162	-0,162	-0,162	-0,162	-0,162	-0,162	-0,162	-0,162	-0,162	-0,216	-0,171	-0,171
10	0	0	0,03	0,1	0,13	0,3	0,3	0,25	0,11	-0,162	-0,162	-0,162	-0,162	-0,162	-0,162	-0,162	-0,162	-0,162	-0,162	-0,216	-0,171	-0,171
12	0	0	0,01	0,06	0,08	0,25	0,25	0,15	0,07	-0,162	-0,162	-0,162	-0,162	-0,162	-0,162	-0,162	-0,162	-0,162	-0,162	-0,216	-0,171	-0,171
15	0	0	0	0,01	0,02	0,14	0,14	0,07	0,03	-0,162	-0,162	-0,162	-0,162	-0,162	-0,162	-0,162	-0,162	-0,162	-0,162	-0,216	-0,171	-0,171
18	0	0	0	0	0	0,09	0,09	0,04	-0,01	-0,162	-0,162	-0,162	-0,162	-0,162	-0,162	-0,162	-0,162	-0,162	-0,162	-0,216	-0,171	-0,171
20	0	0	0	0	0	0,06	0,06	0,02	-0,02	-0,162	-0,162	-0,162	-0,162	-0,162	-0,162	-0,162	-0,162	-0,162	-0,162	-0,216	-0,171	-0,171
25	0	0	0	0	0	0,02	0,02	0	-0,03	-0,162	-0,162	-0,162	-0,162	-0,162	-0,162	-0,162	-0,162	-0,162	-0,162	-0,216	-0,171	-0,171
28	0	0	0	0	0	0,02	0,02	0	-0,03	-0,162	-0,162	-0,162	-0,162	-0,162	-0,162	-0,162	-0,162	-0,162	-0,162	-0,216	-0,171	-0,171
30	0	0	0	0	0	0	0	0	-0,03	-0,162	-0,162	-0,162	-0,162	-0,162	-0,162	-0,162	-0,162	-0,162	-0,162	-0,216	-0,171	-0,171
35	0	0	0	0	0	-0,04	-0,04	0	-0,03	-0,162	-0,162	-0,162	-0,162	-0,162	-0,162	-0,162	-0,162	-0,162	-0,162	-0,216	-0,171	-0,171
90	0	0	0	0	0	-0,04	-0,04	0	-0,03	-0,162	-0,162	-0,162	-0,162	-0,162	-0,162	-0,162	-0,162	-0,162	-0,162	-0,216	-0,171	-0,171

APPENDIX 5

HUYGENS EM UP-DATED AEDB IN TRANSITIONAL FLOW REGIME

Knudsen	0,001	0,002	0,003	0,005	0,007	0,01	0,015	0,02	0,025
Log(Kn)	-3	-2,699	-2,523	-2,301	-2,155	-2,000	-1,824	-1,699	-1,602
C_A(0°)	1,478	1,487	1,499	1,523	1,543	1,568	1,600	1,624	1,645
C_A(5°)	1,457	1,465	1,478	1,502	1,522	1,547	1,579	1,604	1,625
C_A(10°)	1,417	1,426	1,439	1,462	1,483	1,507	1,539	1,564	1,585
C_A(20°)	1,248	1,257	1,269	1,293	1,313	1,338	1,370	1,395	1,416
C_A(30°)	1,066	1,074	1,085	1,105	1,123	1,144	1,172	1,194	1,211
C_N(0°)	0,000	0,000	0,000	0,000	0,000	0,000	0,000	0,000	0,000
C_N(5°)	0,024	0,026	0,028	0,032	0,036	0,041	0,047	0,051	0,055
C_N(10°)	0,057	0,059	0,064	0,072	0,079	0,088	0,099	0,108	0,115
C_N(20°)	0,124	0,129	0,137	0,152	0,165	0,181	0,201	0,217	0,230
C_N(30°)	0,175	0,182	0,193	0,213	0,230	0,251	0,279	0,300	0,317
X_{CP}/L(0°)	0,700	0,675	0,650	0,602	0,561	0,511	0,444	0,392	0,351
X_{CP}/L(5°)	0,694	0,670	0,645	0,598	0,557	0,507	0,441	0,389	0,349
X_{CP}/L(10°)	0,699	0,674	0,649	0,601	0,561	0,510	0,443	0,392	0,351
X_{CP}/L(20°)	0,728	0,702	0,675	0,626	0,583	0,530	0,460	0,407	0,364
X_{CP}/L(30°)	0,765	0,738	0,710	0,658	0,612	0,556	0,483	0,426	0,381
C_{mMRC}(0°)	0,000	0,000	0,000	0,000	0,000	0,000	0,000	0,000	0,000
C_{mMRC} (5°)	-0,010	-0,010	-0,011	-0,011	-0,011	-0,010	-0,008	-0,006	-0,005
C_{mMRC} (10°)	-0,024	-0,024	-0,025	-0,024	-0,023	-0,022	-0,018	-0,014	-0,010
C_{mMRC} (20°)	-0,057	-0,056	-0,056	-0,055	-0,053	-0,048	-0,039	-0,031	-0,023
C_{mMRC} (30°)	-0,088	-0,086	-0,086	-0,084	-0,080	-0,073	-0,061	-0,048	-0,037

AERODYNAMIC COEFFICIENTS IN TRANSITIONAL REGIME

Knudsen	0,04	0,05	0,06	0,08	0,1	0,2	0,3	0,5	0,7
Log(Kn)	-1,398	-1,301	-1,222	-1,097	-1,000	-0,699	-0,523	-0,301	-0,155
C_A(0°)	1,690	1,712	1,731	1,761	1,784	1,856	1,896	1,944	1,973
C_A(5°)	1,671	1,693	1,712	1,742	1,766	1,838	1,879	1,927	1,956
C_A(10°)	1,630	1,653	1,672	1,702	1,725	1,797	1,838	1,886	1,915
C_A(20°)	1,461	1,484	1,503	1,533	1,556	1,628	1,669	1,717	1,746
C_A(30°)	1,251	1,270	1,286	1,312	1,333	1,395	1,430	1,472	1,497
C_N(0°)	0,000	0,000	0,000	0,000	0,000	0,000	0,000	0,000	0,000
C_N(5°)	0,063	0,068	0,071	0,077	0,081	0,094	0,102	0,111	0,116
C_N(10°)	0,131	0,139	0,146	0,156	0,164	0,189	0,204	0,220	0,231
C_N(20°)	0,259	0,273	0,285	0,304	0,319	0,365	0,390	0,421	0,439
C_N(30°)	0,356	0,375	0,391	0,416	0,436	0,497	0,531	0,572	0,597
X_{CP}/L(0°)	0,327	0,315	0,305	0,289	0,276	0,246	0,231	0,215	0,209
X_{CP}/L(5°)	0,325	0,313	0,303	0,287	0,274	0,245	0,229	0,214	0,208
X_{CP}/L(10°)	0,327	0,315	0,305	0,289	0,276	0,246	0,230	0,215	0,208
X_{CP}/L(20°)	0,339	0,326	0,315	0,298	0,284	0,253	0,236	0,220	0,212
X_{CP}/L(30°)	0,354	0,340	0,329	0,311	0,296	0,261	0,244	0,225	0,217
C_{mMRC} (0°)	0,000	0,000	0,000	0,000	0,000	0,000	0,000	0,000	0,000
C_{mMRC} (5°)	-0,004	-0,003	-0,003	-0,002	-0,001	0,002	0,004	0,006	0,007
C_{mMRC} (10°)	-0,008	-0,007	-0,006	-0,004	-0,002	0,004	0,007	0,011	0,013
C_{mMRC} (20°)	-0,019	-0,017	-0,014	-0,010	-0,006	0,005	0,011	0,019	0,023
C_{mMRC} (30°)	-0,032	-0,028	-0,025	-0,019	-0,013	0,002	0,011	0,023	0,029

AERODYNAMIC COEFFICIENTS IN TRANSITIONAL REGIME

Knudsen	0,9	1,23	2	3	5	7	9	10
Log(Kn)	-0,046	0,090	0,301	0,477	0,699	0,845	0,954	1,000
C_A(0°)	1,992	2,015	2,045	2,065	2,081	2,088	2,090	2,090
C_A(5°)	1,976	1,999	2,030	2,049	2,066	2,073	2,075	2,075
C_A(10°)	1,935	1,958	1,988	2,007	2,024	2,031	2,033	2,033
C_A(20°)	1,766	1,789	1,819	1,838	1,855	1,862	1,864	1,864
C_A(30°)	1,514	1,534	1,560	1,577	1,592	1,597	1,599	1,599
C_N(0°)	0,000	0,000	0,000	0,000	0,000	0,000	0,000	0,000
C_N(5°)	0,120	0,124	0,130	0,133	0,136	0,138	0,138	0,138
C_N(10°)	0,238	0,246	0,256	0,263	0,269	0,271	0,272	0,272
C_N(20°)	0,452	0,466	0,485	0,498	0,509	0,513	0,514	0,514
C_N(30°)	0,614	0,633	0,659	0,675	0,690	0,695	0,697	0,697
X_{CP}/L(0°)	0,207	0,209	0,195	0,187	0,186	0,193	0,204	0,211
X_{CP}/L(5°)	0,206	0,209	0,194	0,187	0,186	0,193	0,204	0,211
X_{CP}/L(10°)	0,206	0,209	0,195	0,187	0,186	0,193	0,204	0,211
X_{CP}/L(20°)	0,210	0,212	0,196	0,188	0,187	0,193	0,204	0,211
X_{CP}/L(30°)	0,214	0,215	0,198	0,189	0,187	0,194	0,204	0,211
C_{mMRC} (0°)	0,000	0,000	0,000	0,000	0,000	0,000	0,000	0,000
C_{mMRC} (5°)	0,007	0,007	0,009	0,010	0,011	0,010	0,008	0,007
C_{mMRC} (10°)	0,014	0,014	0,018	0,020	0,021	0,019	0,017	0,015
C_{mMRC} (20°)	0,025	0,025	0,033	0,038	0,040	0,037	0,031	0,028
C_{mMRC} (30°)	0,031	0,031	0,044	0,051	0,054	0,050	0,042	0,038

AERODYNAMIC COEFFICIENTS IN TRANSITIONAL REGIME